Chapter 12: "Post-collisional collapse in the wake of migrating arc-continent collision in the Ilan Basin, Taiwan" (P.D. Clift, A.T.S. Lin, A. Carter, F. Wu, A.E. Draut, T.-H. Lai, L.-Y. Fei, H. Schouten, and L. Teng) in ***SPE436: Formation and Applications of the Sedimentary Record in Arc Collision Zones*** *(A.E. Draut, P.D. Clift, and D.W. Scholl)*

The Geological Society of America
Special Paper 436
2008

Post-collisional collapse in the wake of migrating arc-continent collision in the Ilan Basin, Taiwan

Peter D. Clift
School of Geosciences, University of Aberdeen, Aberdeen, AB24 3UE, UK, and *DFG-Research Centre Ocean Margins (RCOM), Geowissenschaften, Universität Bremen, Klagenfurter Strasse, 28359 Bremen, Germany*

Andrew T.S. Lin
Department of Earth Sciences, National Central University, 300, Jungda Road, Jungli, Taiwan

Andrew Carter
School of Earth Sciences, University and Birkbeck College London, Gower Street, London, WC1E 6BT, UK

Francis Wu
State University of New York at Binghamton, Department of Geological Sciences and Environmental Studies, P.O. Box 600, Binghamton, New York 13902-6000, USA

Amy E. Draut
U.S. Geological Survey, Pacific Science Center, 400 Natural Bridges Drive, Santa Cruz, California 95060, USA

T.-H. Lai
L.-Y. Fei
Central Geological Survey, 2, Lane 109, Hua-Hsin Street, Chung-Ho, Taipei, Taiwan 235

Hans Schouten
Department of Geology and Geophysics, Woods Hole Oceanographic Institution, Woods Hole, Massachusetts 02543, USA

Louis Teng
Department of Geosciences, National Taiwan University, Roosevelt Road, Taipei, Taiwan

ABSTRACT

The Ilan Basin of northern Taiwan forms the western limit of the Okinawa Trough, where the trough meets the compressional ranges of central Taiwan. Apatite fission-track ages of 1.2 ± 0.5 Ma and 3.5 ± 0.5 Ma, measured north and south of the basin, respectively, indicate faster exhumation rates in the Hsüehshan Range to the north (>1.6 mm/yr) than in the Backbone Range to the south (0.7 mm/yr). Reconstructed subsidence rates along the northern basin margin are also faster than in the south (6–7 compared with 3–5 mm/yr). Global positioning system (GPS) and active seismological data indicate motion of the southern basin margin to the east and southeast.

Clift, P.D., Lin, A.T.S., Carter, A., Wu, F., Draut, A.E., Lai, T.-H., Fei, L.-Y., Schouten, H., and Teng, L., 2008, Post-collisional collapse in the wake of migrating arc-continent collision in the Ilan Basin, Taiwan, *in* Draut, A.E., Clift, P.D., and Scholl, D.W., eds., Formation and Applications of the Sedimentary Record in Arc Collision Zones: Geological Society of America Special Paper 436, p. 257–278, doi: 10.1130/2008.2436(12). For permission to copy, contact editing@geosociety.org.

We propose that the Ilan Basin is being formed as a result of extension of northern Taiwan, largely controlled by a major southeast-dipping fault, modeled at ~30° dip, and mapped as a continuation of the Lishan Fault, a major thrust structure in the Central Ranges. Flexural rigidity of the lithosphere under the basin is low, with elastic thickness ~3 km. A southwest-migrating collision between the Luzon Arc and southern China, accompanied by subduction polarity reversal in the Ryukyu Trench, has allowed crustal blocks that were previously held in compression between the Eurasian and Philippine Sea plates to move trenchward as they reach the northern end of the collision zone. Subduction polarity reversal permits rapid extension and formation of the Ilan Basin and presumably, at least, the western Okinawa Trough, as a direct consequence of arc-continent collision, not because of independent trench rollback forces. This conceptual model suggests that migrating arc-continent collision causes the rapid formation of deep marginal basins that are then filled by detritus from the adjacent orogen, and that these should be common features in the geologic record.

Keywords: collision, extension, erosion, subduction, seismology.

INTRODUCTION

The Earth's continental crust is generally considered to be largely generated by magmatism along active plate margins, a process that balances the long-term loss of continental crust back into the mantle through subduction zones (e.g., von Huene and Scholl, 1991; Rudnick and Fountain, 1995; Clift and Vannucchi, 2004). This balance is maintained because arc crust generated in oceanic subduction settings is not entirely subducted when these features collide with other trench systems or passive continental margins. Instead, continental masses appear to be built up as a result of the progressive accretion of primitive arc blocks to older, preexisting continental blocks. Understanding the tectonism of arc-continent collision is important, not only because this process is fundamental to the conservation of the total volume of continental crust, but also because it is likely the most important method by which active continental margins are created (e.g., Casey and Dewey, 1984; Konstantinovskaya, 1999).

Accreted oceanic island-arc terranes have been recognized in a number of orogenic suture zones (e.g., Kohistan in the Himalaya, Talkeetna in southern Alaska, South Mayo in the Irish Caledonides), and the process of arc-continent collision forms an inevitable part of the plate tectonic cycle. Arc-continent and continent-continent collisions are unlikely to be identical because of the different mechanical properties of arc and cratonic lithospheres. In this paper we investigate the later stages of arc-continent collision, specifically the collapse of the collisional mountain belts to form sedimentary basins whose fill might be used to understand the collision process.

In order to understand the collapse of arc collisional mountains, we examine the Ilan Basin of northern Taiwan. Taiwan, located off the coast of southeastern China, comprises some of the tallest and most rapidly uplifting and eroding mountains in East Asia. The orogen is formed by the collision between the oceanic Luzon Arc and the passive margin of southern China (Suppe, 1981; Chemenda et al., 1997), which is itself built on the remains of a Cretaceous continental arc (Davis et al., 1997). The collision between the Luzon oceanic arc and mainland Asia is oblique, so that the collision point must have migrated along the Asian continental margin through time. At any given time the north end of the island will represent arc units and Chinese passive-margin sequences that began to be involved in collision earlier than those in the south, where collision is just starting. Thus northern Taiwan is the optimal place to examine the processes that occur during and after the peak of arc-continent collision. These processes form the subject of this paper.

Radiometric dating of the metamorphic rocks exposed in the Central Ranges, combined with biostratigraphic dating of orogenic sediment from the Coastal Ranges, indicates that collision of this part of the Luzon Arc with mainland Asia started ca. 6–9 Ma (e.g., Suppe, 1981; Teng, 1990; Sibuet et al., 2002; Malavieille et al., 2002; Huang et al., 2006). A wide consensus in the community agrees that Taiwan represents a simple collision between the Luzon Arc and mainland Asia, an assumption that underlies this present study. Nonetheless, we note that alternative models have been advanced to explain the mountain building. One theory involves collision of an exotic terrane with the Chinese passive margin, followed by later collision of the Luzon Arc (Lu and Hsü, 1992). Another model invokes compressional tectonism following collision of the Luzon Arc with the Ryukyu Arc, which would previously have extended farther southwest along the southern margin of China (Hsu and Sibuet, 1995; Sibuet and Hsu, 1997).

It is unclear when the collision between Luzon and Eurasia began. Whereas some models favor collision to have initiated only ca. 6–9 Ma, effectively just to the east of the present collision zone (e.g., Suppe, 1984; Sibuet and Hsu, 1997; Huang et al., 2000, 2006), other models suggest a more steady-state collision that may have started earlier (e.g., Suppe, 1984; Teng, 1990, 1996; Clift et al., 2003). In the steady-state model the modern collision represents a snapshot of a continuous collision process that is migrating to the southwest along the Chinese margin, accreting at least part of the crust of the Luzon Arc to the edge of Eurasia, while generating a new Ryukyu Arc-Trench system and associated Okinawa Trough in its wake. Debate continues as to whether the Okinawa Trough is an active rift system formed by trench tectonic forces linked to the Ryukyu subduction zone and propagating to the southwest into the northern tip of the Taiwan orogen (e.g., Suppe, 1984; Sibuet et al., 1998; Wang et al., 1999), or whether it represents the product of gravitational collapse of the Taiwan orogen, following subduction polarity reversal (e.g., Teng, 1996; Clift et al., 2003). In the latter case, extension of the Ilan Basin has occurred because of the reversal of subduction polarity following arc-continent collision, which removes the stresses that support the high topography in central Taiwan. The earliest phases of extension form the Ilan Plain Basin. The Okinawa Trough represents the continuation of this extension to form a deep marine basin offshore. Without the tectonic push from the Philippine Sea plate the orogen is able to extend because of the free edge provided by the new trench. Specifically, there is no need for slab break-off to allow polarity reversal or as a trigger of orogenic extension.

REGIONAL GEOLOGY

The Ilan Basin forms the onshore western limit of the Okinawa Trough and lies in northeast Taiwan (Figs. 1 and 2). The basin is supplied with sediment from the southwest via the Lanyang River. This river terminates in a small delta, facing into the deeper waters of the Okinawa Trough. To the north the basin is bounded by exposures of shale and sandstone of the Meichi, Szeleng, and Chiayang Formations, which are dated as Oligocene, and typically interpreted to be part of the passive margin of China (Suppe, 1981; Teng, 1990; Lundberg et al., 1997), as well as minor amounts of the underlying Eocene Tachien Sandstone, which represents a synrift deposit, predating Oligocene seafloor spreading (Fig. 3). The whole sedimentary sequence was deformed and thrust to the northwest during the Taiwan orogeny, forming the

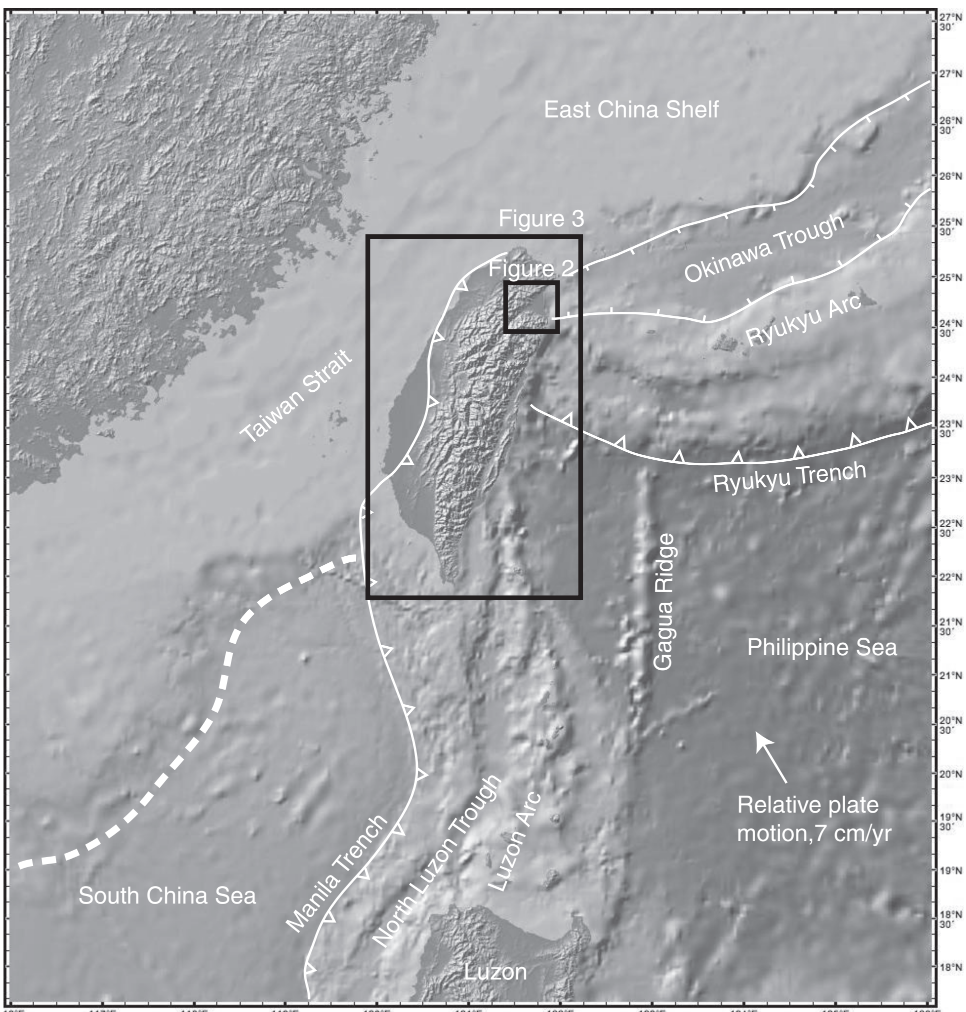

Figure 1. Regional bathymetric map of the Taiwan region, showing the collision between the Luzon Arc and the passive margin of southern China. The Okinawa Trough is in active extension to the east of Taiwan, and its western end comes onshore in the Ilan Plain. Dashed white line marks the base of the continental slope in the South China Sea.

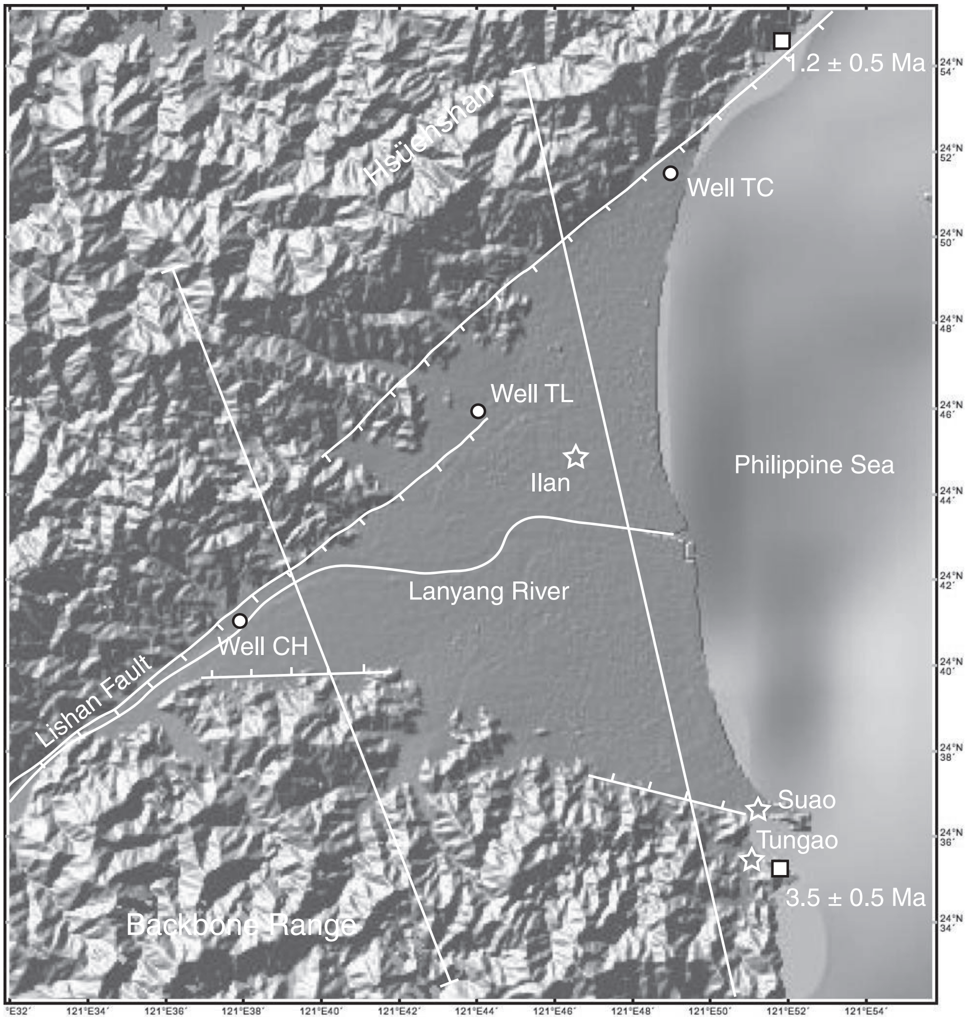

Figure 2. Shaded topographic map of the Ilan Plain area, showing the location of the drill sites considered in this study, the position of apatite fission-track samples (with average age of the dominant population), and the orientation of topographic profiles shown in Figure 5. Map is from NASA Shuttle Radar data, made available through www.geomapapp.org.

modern Hsüehshan Range. Peak metamorphic grades are low (e.g., Chen, 1984). Liu et al. (2001) used zircon fission-track data to show that these units had not been buried beyond the partial annealing temperature for that mineral (~200 °C; Tagami et al., 1998) and inferred a lower greenschist metamorphic facies.

The southern edge of the basin is marked by outcrops of the shale-rich Miocene Lushan Formation, which Liu et al. (2001) considered to have reached prehnite-pumpellyite facies, and thus is of a slightly lower grade than the Hsüehshan Range. The Lushan Formation makes up much of the Backbone Range and unconformably overlies the Tananao Schist locally (Suppe et al., 1976), which is formed largely of Paleozoic and Mesozoic sedimentary rocks, metamorphosed to greenschist grade. The oldest sedimentary rocks overlying the Tananao Schist are Eocene conglomerates of the Pilushan Formation, but the onlap is time transgressive between basin and highs on the paleo-Chinese margin. Localized slices of higher grade Tananao metamorphic rocks, including mafic amphibolites, are well exposed on the coast at Tungao, south of Suao (Chen and Jahn, 1998). The Tananao Schist is dated to have been metamorphosed during the Mesozoic and subsequently overprinted by greenschist conditions in the Pliocene (Lo and Yu, 1996; Wang et al., 1998).

Southwest of the Ilan Basin the Lushan and Tatungshan Formations are juxtaposed across the Lishan Fault. In central Taiwan the Lishan Fault is manifested as a major, steep, NW-dipping thrust structure, having an ESE-vergent geometry, interpreted by Clark et al. (1993) as an antithetic backthrust relative to the dominant northwest-vergent thrust stack in the Central Ranges (Wu, 1978). Changes in stratigraphic thickness across the fault suggest that it is a reactivated structure that originally formed within an extensional rift structure on the South China Sea passive margin (Teng et al., 1991).

NEOTECTONICS OF THE LISHAN FAULT

Although the Lishan Fault is a NW-dipping thrust in central Taiwan, it can be readily traced northward to the SW apex of the Ilan Plain. In this region the fault is overturned and has an extensional sense of motion at the western limit of the Ilan Basin, meaning that the slip sense remains the same. The Lishan Fault is

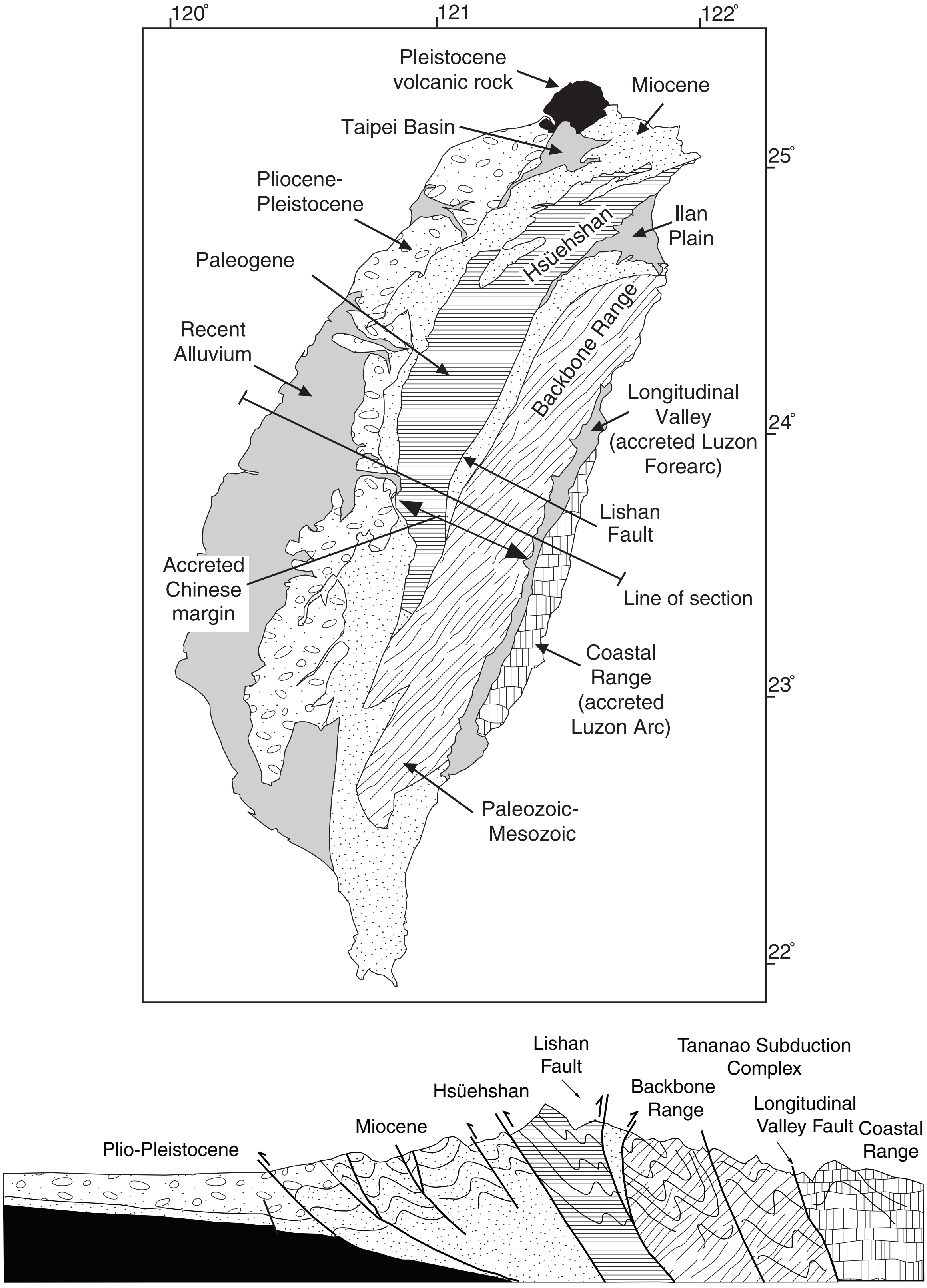

Figure 3. Simplified geological map of Taiwan, showing the map tectonic units that constitute the island and the location of the Ilan Basin along the strike of the Lishan Fault, which separates the Hsüehshan and Backbone Ranges. The lower cross section is modified from Lee et al. (2002) and shows the large-scale structure of the thrust belt in central Taiwan and the geometry of the Lishan Fault, which subsequently has become the dominant structure of the Ilan Plain Basin.

such a major tectonic division that it can be readily traced to pass from being a thrust in central Taiwan to an extensional fault in the Ilan Plain (Teng and Lee, 1996). In the western Ilan Basin the Lishan Fault forms a normal fault of relatively high angle (>60°) that separates the Hsüehshan Range from the Pleistocene basin fill (Teng and Lee, 1996). The topographic break along the northern edge of the basin is commonly sharp and suggestive of an active neotectonic structure (Fig. 4A; Shyu et al., 2005). Exposures of the sedimentary rocks that form the Hsüehshan Range are relatively fresh and prominent at the northern edge of the basin along much of its length. Figure 4B shows an example of well-bedded, relatively unweathered sedimentary rocks, exposed close to the trace of the fault near the southwestern end of the basin. In this area the southern boundary of the basin is also sharp and consistent with neotectonic faulting, as shown in map view (Fig. 2) and in topographic profiles drawn across the strike of the basin (Fig. 5). However, the shaded topographic map (Fig. 2) also shows that the southern basin margin is less linear and poorly

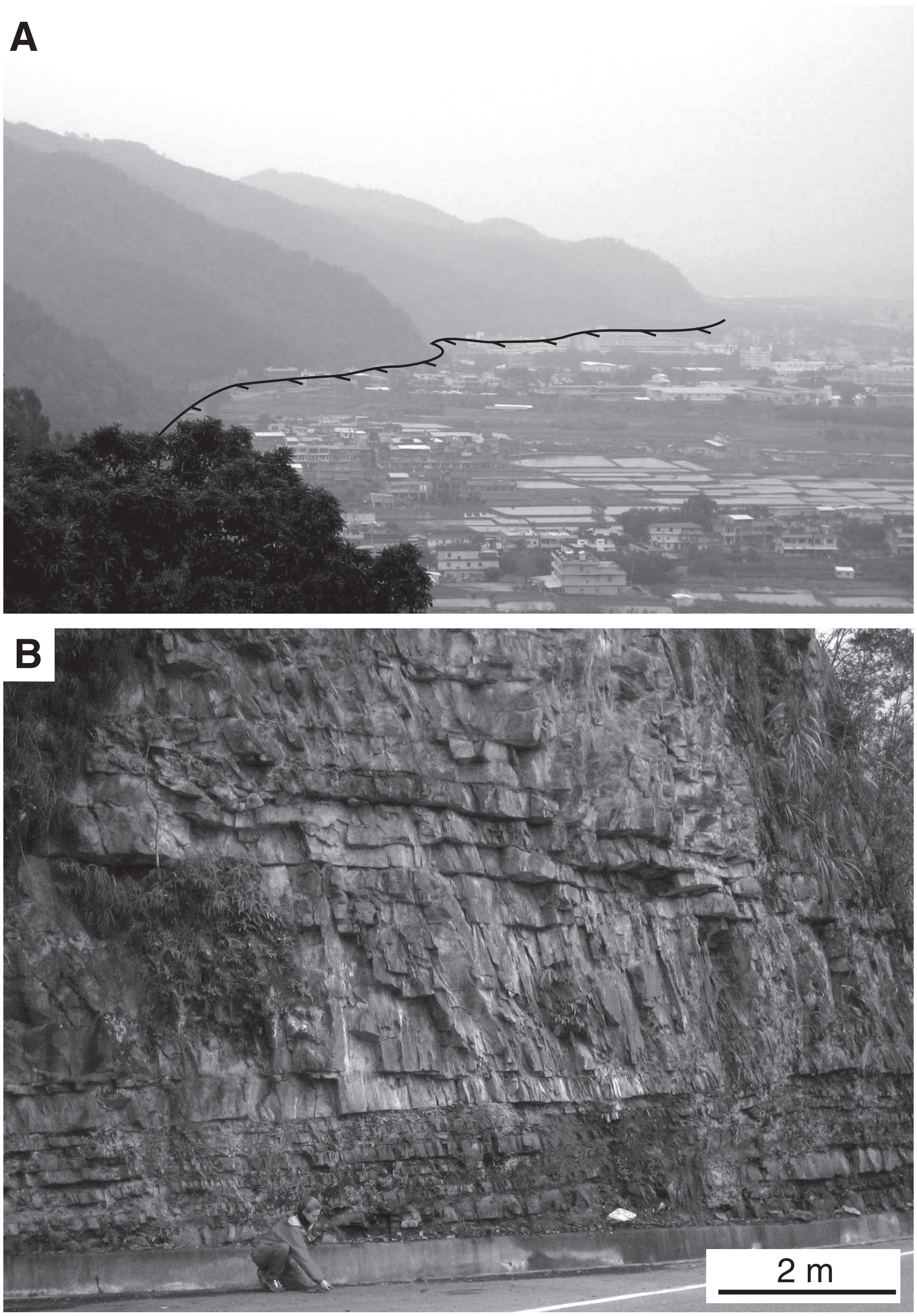

Figure 4. Field photographs. (A) Steep escarpment along the northeast edge of the Ilan Plain, testifying to the fault-bounded nature of the boundary. (B) A relatively fresh exposure of sandstone and shale exhumed by the Lishan Fault at the western end of the Ilan Plain, testifying to the recent activity of the fault along the northern edge of the basin.

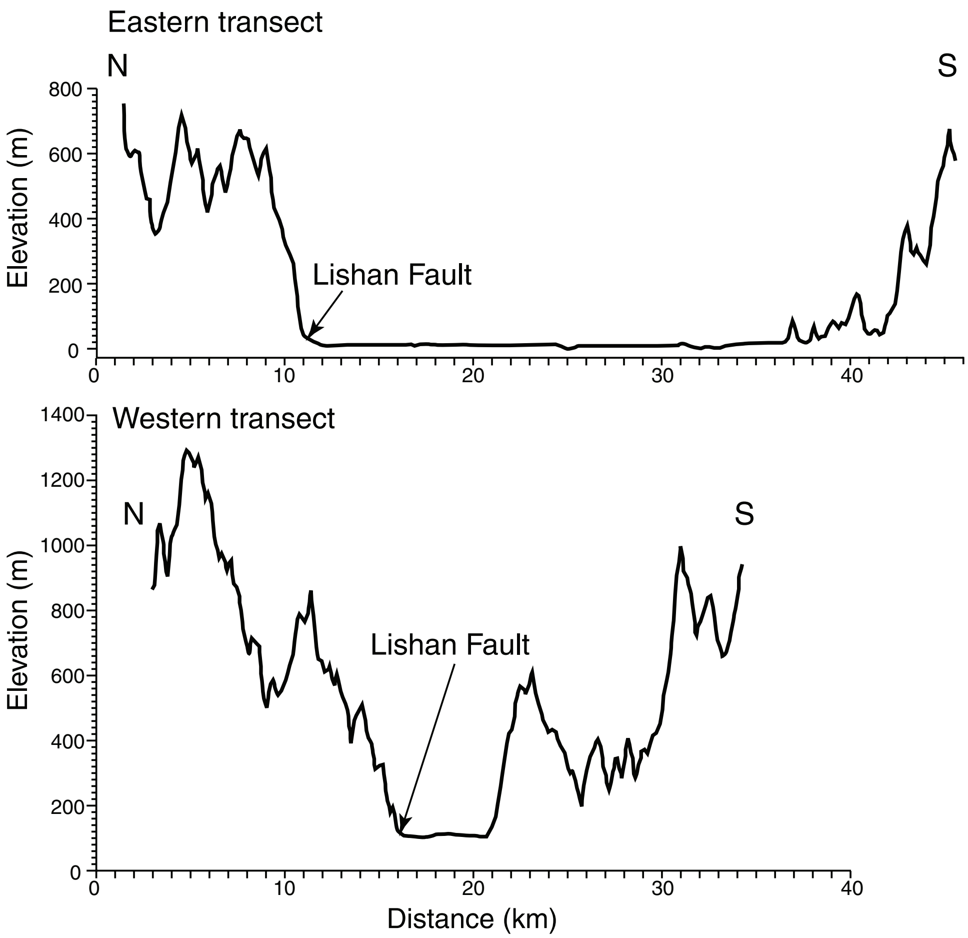

Figure 5. Topographic profiles across the Ilan Plain Basin, showing the asymmetry of the basin margins, especially in the east, where the northern, fault-controlled margin rises rapidly owing to unloading along the Lishan Fault.

defined in comparison with the northern boundary. Exposures along the southern basin margin are generally not fresh but show strong deep weathering of the basement, inconsistent with recent tectonic exhumation. The eastern part of the plain in particular shows a strong topographic contrast between a gently sloping southern margin and a steep northern margin (Fig. 5).

This general contrast between the northern and southern expressions of the Lishan Fault suggests that the northern boundary is mostly fault controlled. However, the relationship is less clear in the south and is more consistent with erosion of a tilted hanging block rather than an uplifted footwall block. Although Shyu et al. (2005) proposed a neotectonic fault along the easternmost part of the southern boundary, it is noteworthy that this feature has little topographic expression, suggesting that motion on this structure is rather less than on the Lishan Fault. Sharp increases in topographic gradient within the Backbone Range south of the basin boundary nonetheless indicate that faulting is active in this region.

Although the eastern and western ends of the northern margin of the Ilan Basin are well defined, and apparently fault-controlled, these trends do not align with one another but instead are separated by a section ~10 km wide with less topographic relief (Fig. 2). We infer a relay section in the Lishan Fault extension in this area, where motion is transferred laterally. As is often the case in fault relay zones in rifts, this area is marked by rivers that enter the basin laterally, adding to the sediment provided by the axial Lanyang River (e.g., Leeder and Gawthorpe, 1987).

DRILLING CONSTRAINTS ON NEOTECTONISM

Drilling by the Central Geological Survey of Taiwan has allowed the basement contact along the faulted northern edge of the Ilan Basin to be determined at depth as well as at outcrop. Cores from three sites were examined in this project, wells TC, TL, and CH, trending east to west close to the northern edge of the basin (Fig. 2). These wells intersect the basement at depths of 17, 84, and 38 m, respectively, suggesting an average dip of the basement-cover interface under the northern edge of only ~10°, although this is over a short distance and may not be representative of the dip over the whole basin width. The overlying sediment comprises sequences of alluvial, coastal, and some shallow marine sediment that has been dated as late Pleistocene to Holocene by AMS ^{14}C methods (Lai and Hsieh, 2003). The sediment recovered at well CH includes fine-grained muds, silts, and fine sands but is dominated by thick-bedded debris-flow gravels, with clasts up to 10 cm across (Fig. 6). Well TL recovered the finest

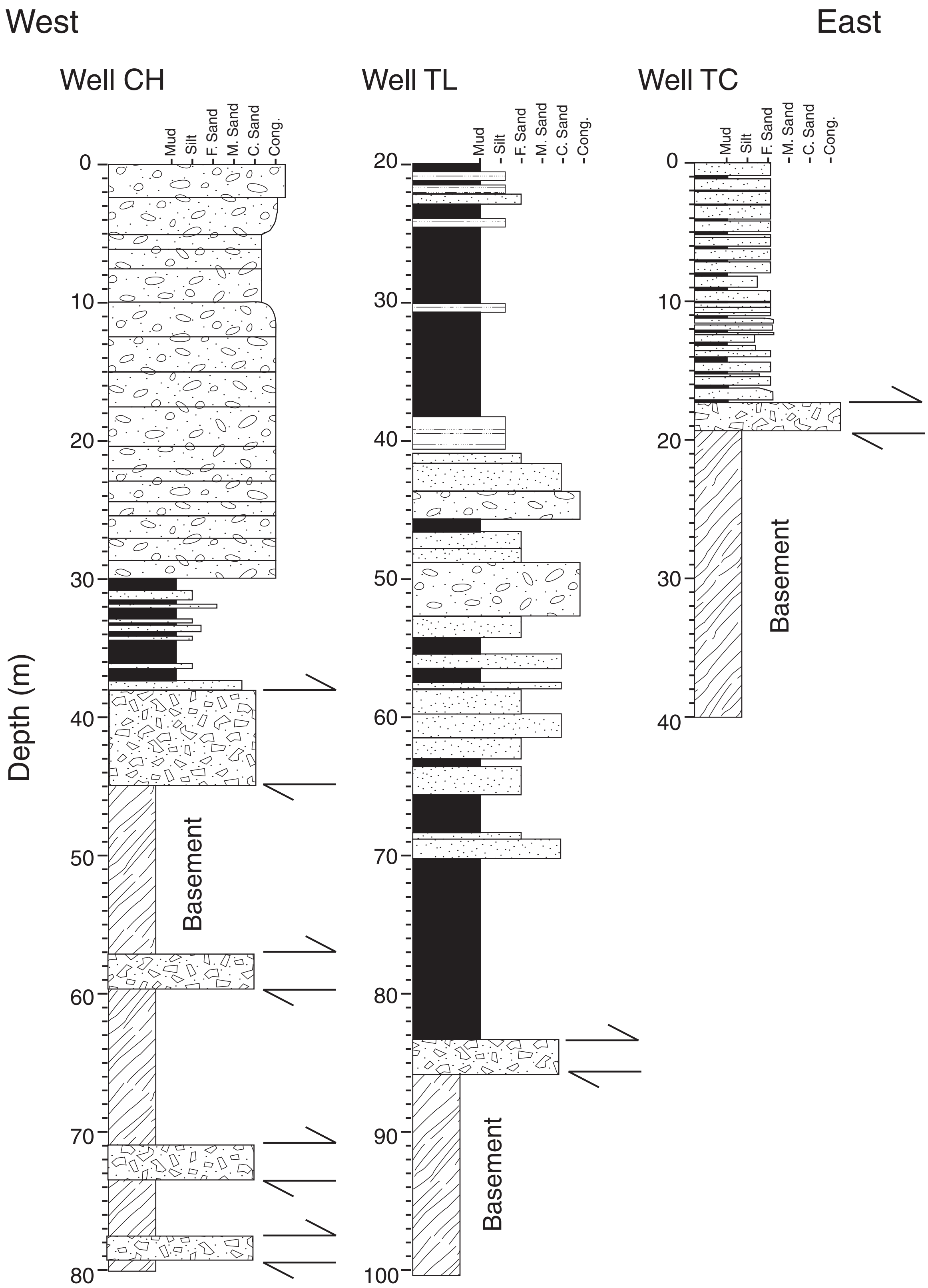

Figure 6. Sedimentary logs showing the cored sequences found along the northern edge of the Ilan Plain, where Pleistocene sediment is deposited over low-grade metamorphosed sedimentary rock, commonly below a zone of fault breccia that marks a detachment surface.

grained sand of the three drilled sequences, though the sediment is still characterized by coarse sands and gravels. Well TC recovered a sequence of medium- to thick-bedded sands and muds. In each location the sediment is underlain by well-lithified, low-grade metamorphosed shale, typical of that seen in outcrop in the Hsüehshan Range.

All drilled basement samples are distinguished by the presence of discrete brecciated layers, generally 2–5 m thick at the basement contact but also present within the basement below that level. These breccias are monomict and comprise only fragments of metamorphosed shale (Fig. 7). The lack of material in the breccias from the shallower basin fill sediment probably reflects the fact that they are loose, unconsolidated materials and unable to support the confining stresses needed to be incorporated into the gouge. Texturally the breccias are generally very angular, unsorted, and matrix supported. The breccias are relatively well lithified in comparison with the overlying soft Pleistocene sediment. We interpret these rocks to represent fault breccias formed by cataclasis in the shallow subsurface of the Lishan Fault. The brittle, angular, broken character of the fault-breccia clasts is apparent in thin section. Critically, the fault breccias postdate the development of cleavage in the metapelites that form the footwall (Fig. 8). As a result, motion on the fault is constrained to being post–peak metamorphism and relatively shallow (<8 km) in the crust. The breccias are preferentially formed close to the basement contact, because this is the fault plane exposed to the surface by the exhumation of the footwall block. Not all the breccia and fault layers lie exactly along the basement-sediment contact, indicating that the Lishan Fault has been active along several fault splays within the footwall block during uplift of the Hsüehshan Range. The drill data confirm the presence of a major southeast-dipping structure that controls the basin's northern margin (Fig. 9).

Because the sediment cored in the Ilan Basin is all close to sea level and preserves evidence of the environment of its sedimentation, these materials can be used to determine rates of tectonic subsidence across the plain. In the Ilan Basin the fast rate of the sediment supply, largely from the Lanyang River, appears generally to match rates of basement subsidence, keeping the basin full while allowing shoreline progradation toward the Okinawa Trough. Lai and Hsieh (2003) demonstrated that subsidence reaches a maximum rate of ~19 mm/yr around the mouth of the Lanyang River and decreases toward the edges of the plain, both north and south, as well as toward the west. However, what is important toward understanding the tectonics of the Ilan Basin is the recognition that the northern part of the plain subsides faster than the southern sector, reaching average Holocene rates of 6–7 mm/yr versus 3–5 mm/yr. This disparity is consistent with the observations presented above that indicate a dominant asymmetric character to the basin structure. We thus favor basin formation above a dominant south-dipping extensional detachment (Fig. 9).

MODELING BASIN GEOMETRY

The large-scale structure of the basin can be considered and modeled using a theoretical forward of an asymmetric basin, controlled by a dominant detachment. We employed the flexural cantilever model of Kusznir et al. (1991) to forward model the deformation and subsidence that would be expected to result from the extension measured across the normal fault that bounds the northern edge of the basin, and to test the idea that the regional dip is 10°, as inferred from the drilling. Although the flexural cantilever model is not the only, or universally accepted, theoretical model for extensional basins, it does have a number of

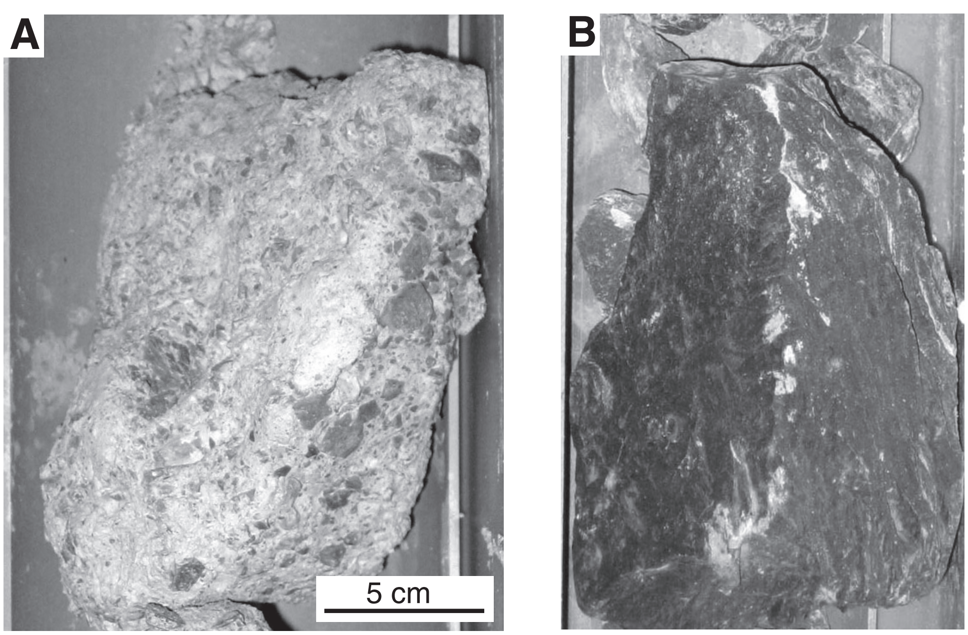

Figure 7. Photographs of cored pre-Pleistocene rocks from well CH in the western Ilan Basin. (A) Fault-brecciated zone at 75.78 m depth. (B) Coherent block of metapelite from 84.50 m depth.

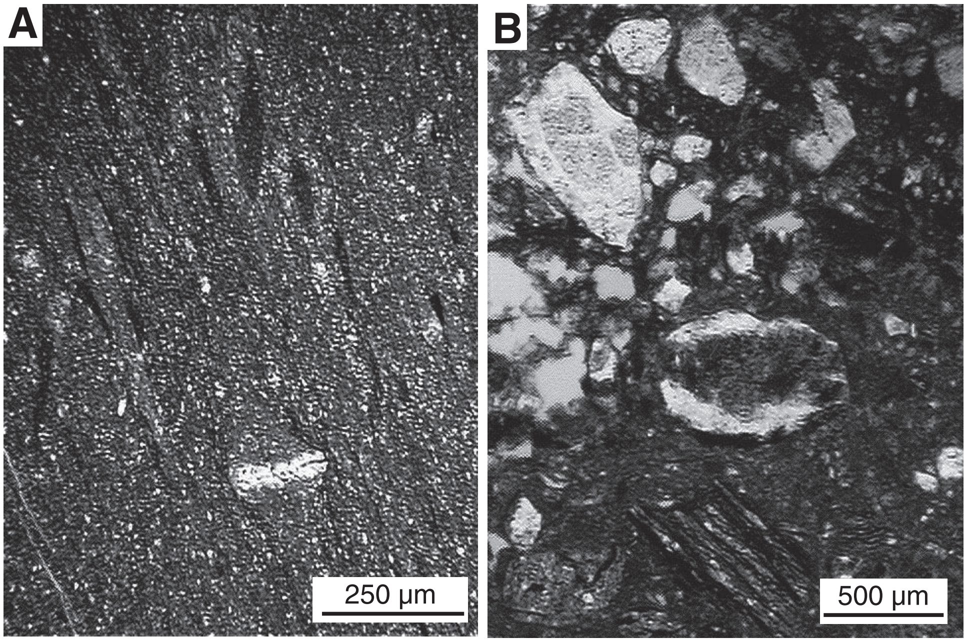

Figure 8. Photomicrographs of thin sections cut from basement rocks in well CH. (A) Typical fine-grained character of the basement metapelites, with a well-developed cleavage. (B) Fault rock from within one of the breccia zones, demonstrating low-temperature shattering textures.

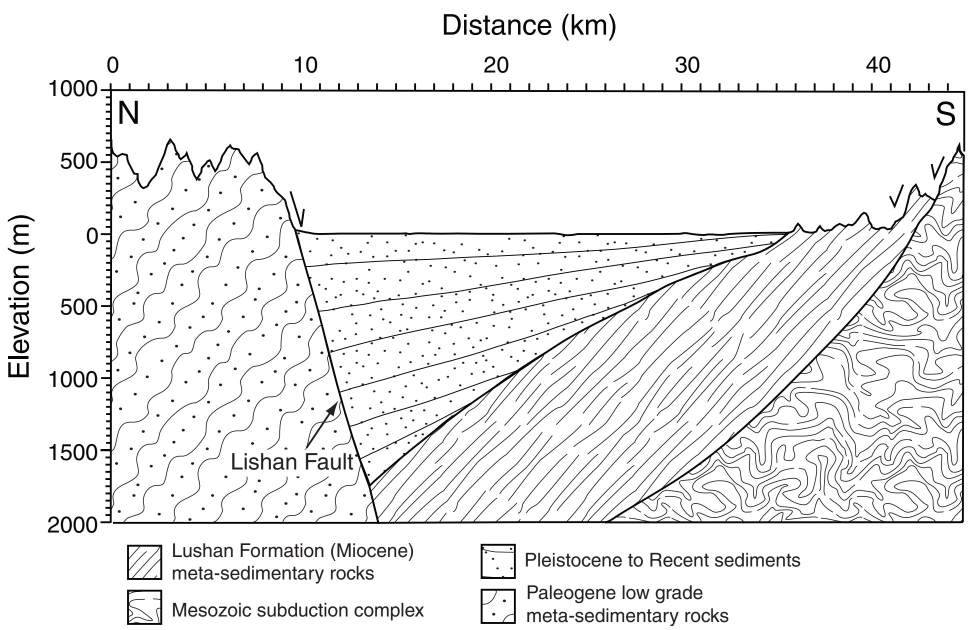

Figure 9. Schematic cross section of the regional basin structure through the eastern Ilan Basin, showing the dominant control of a south-dipping detachment in controlling uplift of the Hsüehshan Range and preferential subsidence of the northern plain. Shading patterns are not intended to accurately portray deformation structures in the footwall and hanging-wall blocks.

important features that allow the basin tectonics to be understood at a first-order level, and it has been used to effect in understanding basins in several parts of the world (Kusznir et al., 1995; Roberts et al., 1993).

The model is complicated by our lack of subsurface data and constraint on the degree of extension across the fault, although this is also limited by the total size of the basin. For modeling purposes we chose a default of 5 km horizontal extension and a crustal thickness of 40 km. In this approach we made no attempt to replicate the basin morphology but simply extended a model continental lithosphere using the major detachment fault and predicted what sort of basin this would form. Flexural rigidity is expected to be low in an arc orogenic setting. Effective elastic thickness (Te) is only 13 km in the Taiwan foreland (Lin and Watts, 2002) and is expected to be rather less in the orogenic core that we consider here. The deformation in the flexural cantilever model assumes brittle faulting in the upper crust, set at 10 km thickness here, and ductile deformation distributed in a sinusoidal fashion over a wavelength of 100 km. The results of the models are shown in Figure 10.

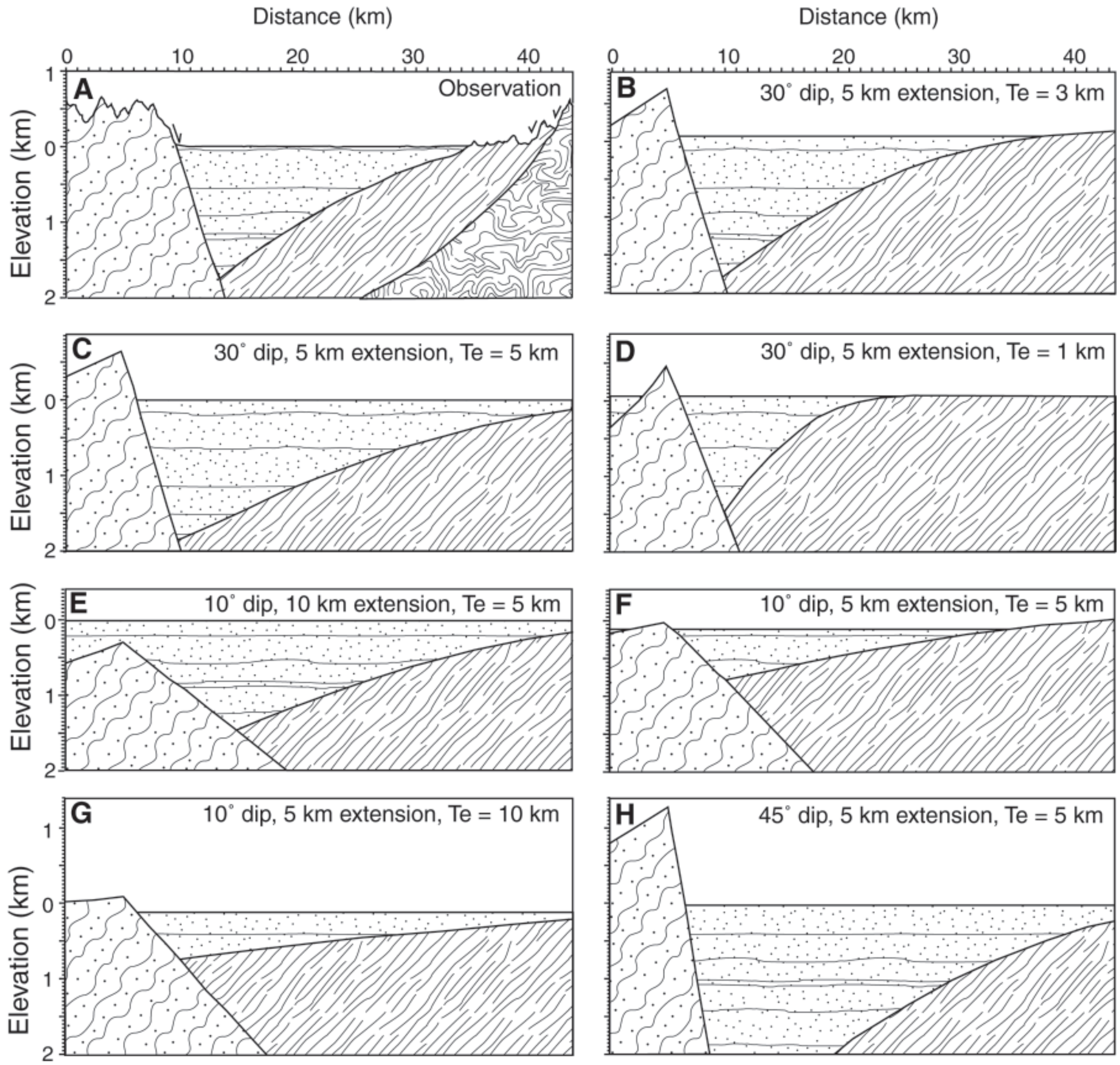

Figure 10. Proposed basin geometries and comparisons with possible model basins in order to limit the possible faulting geometries and strength of the lithosphere under the Ilan Plain. (A) Proposed basin cross section inferred from outcrop, coring, and gravity constraints. (B–D) Forward models, made using the flexural cantilever model of Kusznir et al. (1991) and a 30° detachment fault, with variations in the flexural rigidity of the lithosphere. (E–G) Forward models using a 10° detachment fault, showing the effects of varying amounts of extension and flexural rigidity. (H) Forward models using a 45° detachment fault, showing a poor match to observed basin shape. Te—elastic thickness.

An important result of our forward models is that basins generated above a 10° detachment surface do not produce realistic basin geometries (Fig. 10A, E–G), mostly because they do not predict significant footwall uplift of the size seen in the Hsüehshan. Also, 10° detachments fail to produce footwall uplift even when Te is increased to 10 km (Fig. 10A, G), or if the extension across the fault is increased to 10 km. We conclude that the 10° dip inferred from coring cannot be representative of the basin. The best first-order fit to basin geometry was acquired using a 30° detachment, with a 5 km extension and a Te of 3 km (Fig. 10A, B). Although this is not a unique solution, it does give some guidance as to the type of fault and mechanical state of the crust under the Ilan Plain. Changing flexural rigidity to either 1 km or 5 km changed the basin width to less close fits (Fig. 10A, C, D). The modeling is also effective at eliminating very high angle faults as possible mechanisms, because even a 45° fault produces too much footwall uplift, hanging-wall subsidence, and a wide basin (Fig. 10A, H).

FISSION-TRACK ANALYSIS

The exhumation history of the ranges around the Ilan Basin can be examined using low-temperature thermochronometry. Although previous studies have used fission-track methods in the central parts of Taiwan (e.g., Liu et al., 2000, 2001; Willett et al., 2003), no similar studies around the Ilan Basin have been undertaken. Liu et al. (2001) used zircon fission-track methods to date the cooling history and included a transect north of the basin, across the Hsüehshan Range. Fission-track studies in zircon grains record cooling through a partial annealing zone of 200–320 °C (Tagami et al., 1998), and so this method is sensitive to exhumation driven by erosion and has been widely used in orogenic exhumation studies. However, Liu et al. (2001) recorded zircon fission tracks north of the Ilan Basin that are mostly older than the Taiwan orogeny. Central ages are as low as 22 Ma close to the topographic front of the Hsüehshan Range but become older farther north, consistent with more exhumation at the margin of the basin (Liu et al., 2001). That the zircon fission tracks are this old indicates that they have been partially but not fully reset by late Miocene–Holocene collision-related burial. A lower temperature thermochronometer is thus required to reconstruct the cooling of rock units in shallower parts of the crust.

In this study we employed the fission-track method applied to apatite, which records cooling through ~125–60 °C over time scales of 1–10 m.y. (Green et al., 1989). Apatite fission-track analysis was performed at University College, London, UK. Polished grain mounts were etched with 5N HNO_3 at 20 °C for 20 s to reveal the spontaneous fission tracks. Subsequently, the uranium content of each crystal was determined by irradiation, which induced fission of ^{235}U. The induced tracks were registered in external mica detectors. The samples for this study were irradiated in the thermal facility of the Hifar Reactor at Lucas Heights, Australia. The neutron flux was monitored by including Corning glass dosimeter CN-5, with a known uranium content of 11 ppm, at either end of the sample stack. After irradiation, sample and dosimeter mica detectors were etched in 48% HF at 20 °C for 45 min. Only crystals with sections parallel to the *c*-axis were counted, as these crystals have the lowest bulk etch rate. To avoid biasing results through preferred selection of apatite crystals, the samples were systematically scanned, and each crystal encountered with the correct orientation was analyzed, irrespective of track density. The results of the fission-track analysis are presented in Table 1.

Of 12 samples analyzed, only 2 yielded sufficient apatite to produce meaningful results. Fortunately these samples came from opposite sides of the basin (Fig. 2) and allow the exhumation histories of the margins to be compared. Central ages of 1.2 ± 0.5 Ma and 3.5 ± 0.5 Ma were recorded at the coast on the north and south basin margins, respectively (Fig. 11). The southern sample contains a minor number of older grains (older than 150 Ma), reflecting an earlier phase of cooling. However, for this study we focus on most of the population, which records cooling linked only to Pliocene–Holocene tectonism. The single, young grain population seen on the northern margin indicates total resetting and recent, rapid cooling. Exactly why the southern margin sample contains a few grains that are not reset at 3.5 Ma is not clear. However, the vast majority of grains in that sample show a well-defined 3.5 Ma cooling trend (Fig. 11). The spread of ages would be greater if only partial annealing had occurred. We conclude that the sample underwent rapid cooling through the AFTA annealing temperature zone ca. 3.5 Ma. Our result indicates more recent cooling of the north margin in comparison with the south, as might be expected for an asymmetric basin controlled by a south-dipping detachment. What is surprising is that this result is the opposite of Liu et al.'s (2001) zircon fission-track result that has central ages of only 1.5 ± 0.3 Ma in the south close to Suao and 22.2 ± 2.3 Ma along the northern margin, which would imply the opposite sense of motion. Such motion is not consistent with the structural asymmetry presented above. Although the apatite and zircon results are consistent in the north, it is impossible to have younger fission-track ages for zircon than for apatite, calling into question whether the zircon or apatite data from Suao are representative of the region. Assuming a geothermal gradient of 30 °C/km (Barr and Dahlen, 1988; Willett et al., 2003), the apatite data imply average exhumation rates of 1.6 ± 0.3 km/m.y. in the north and 0.7 ± 0.1 km/m.y. in the south. Because we demonstrate the importance of extensional motion on the Lishan Fault in generating uplift of the Hsüehshan Range, much of the exhumation on the north margin may be linked to tectonic unroofing by detachment faulting rather than by erosion.

SEISMIC EVIDENCE

Observation of recent earthquakes is important to understanding the neotectonic evolution of the Ilan Basin, as they provide a measure of where faulting is active and a snapshot of the current stress regime. The seismicity used here is a subset of

TABLE 1. FISSION-TRACK ANALYTICAL DATA

Sample no./ field no.	Mineral	No. of crystals	Dosimeter		Spontaneous		Induced		Age dispersion		Central age (Ma) ±1	Age components		
			ρd	Nd	ρs	Ns	ρi	Ni	$P\chi^2$	RE%		mode 1 (number of grains)	mode 2 (number of grains)	mode 3 (number of grains)
TW114-1	Apatite	30	1.387	3845	0.185	141	3.639	2952	0.0	260.4	**14.4 ± 7.0**	3.5 ± 0.5 (26)	22 ± 12 (2)	294 ± 78 (2)
TW116-3	Apatite	15	1.387	3845	0.009	13	1.666	2116	19.8	97.0	**1.2 ± 0.5**	Single pop		

Note: (i) Track densities are ($\times 10^6$ tr cm^{-2}) numbers of tracks counted (N) shown in parentheses; (ii) analyses by external detector method using 0.5 for the 4π/2π geometric correction factor; (iii) ages calculated using dosimeter glass CN-5; (apatite) ξ_{CN5} = 338 ± 4; CN-2; (zircon) ξ_{CN2} = 127 ± 5 calibrated by multiple analyses of IUGS apatite and zircon age standards (see Hurford, 1990); (iv) $P\chi^2$ is probability for obtaining χ^2 value for v degrees of freedom, where v = no. crystals – 1; (v) central age is a modal age, weighted for different precisions of individual crystals (see Galbraith, 1990).

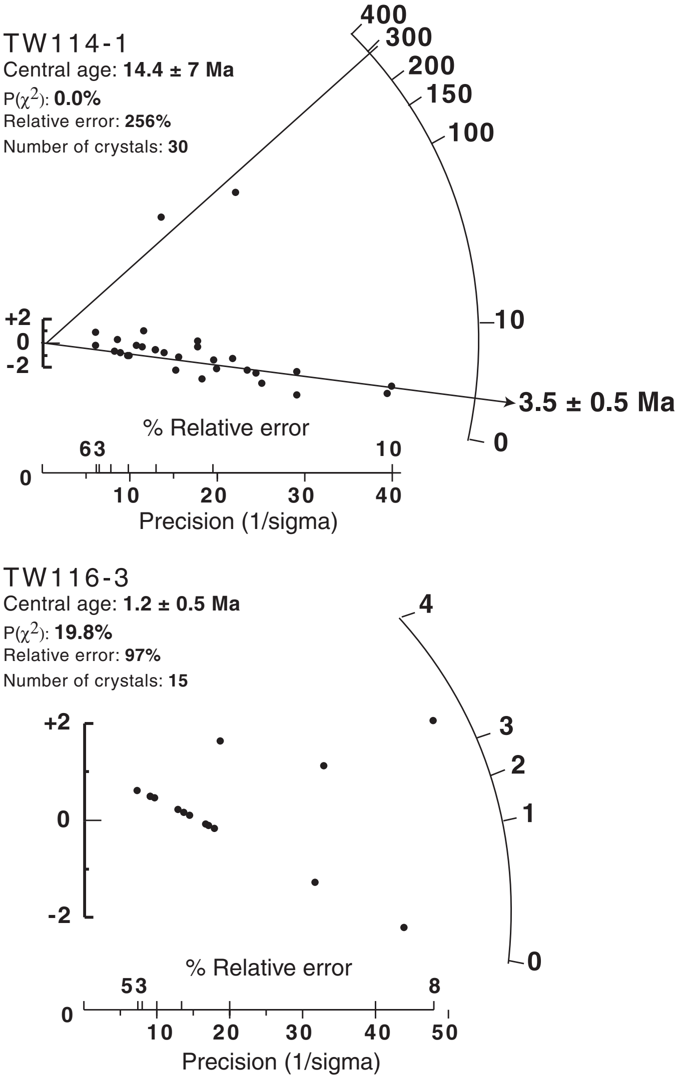

Figure 11. Radial plots of apatite fission-track analyses from Samples TW114-1 and TW116-3, respectively, from the southern and northern margins of the Ilan Basin. Locations shown in Figure 2.

events initially reported by the Central Weather Bureau of Taiwan. The phase data for these events are used for relocation by means of the double-difference method of Waldhauser and Ellsworth (2000). The relocation procedure minimizes the errors in hypocentral determination because of lateral velocity variations. The resulting events tend to cluster around known structures, as shown by Waldhauser (2001).

The Benioff zone in this area is below 50 km and strikes nearly E-W and dips at ~30° to the north (Fig. 12; Wu et al., 1997). In the Ilan area the deeper seismicity (~50 km) is concentrated along the southwestern margin of the basin, as well as more generally across the northern half of the basin. The seismicity in the upper 50 km is shown in Figure 13. Cross sections through the basin show that the deeper earthquakes form a NW-dipping array (Fig. 14A–C). However, a coherent array of deep earthquakes is not seen under the western Okinawa Trough in the 0–50 km depth range considered here. Our deeper profile (Fig. 12) indicates that the Philippine oceanic slab is deeper in this location and that therefore the array of seismic events seen in Figure 14A–C reflects a separate lithospheric structure. The NE-trending seismic zone in the central part of the Ilan Plain is populated by shallow normal-faulting events with NW-SE directed T-axes (extension). In the southeast basin, shallow seismicity appears to be arranged into two shallow E-W–trending zones dominated by sinistral strike-slip events and N-S–oriented normal faulting, but with T-axes in the same general direction as in the basin center. The two areas of intense seismicity are not that different in that both show a shallow layer of seismicity between a narrow range of 8–13 km. Analysis of the map and sections in Figures 13 and 14 reveals the subtle differences in seismicity associated with different belts. In the first place, the shallow events are concentrated in a fairly narrow depth range. This is curious; one possible explanation is that the seismic layer is limited on its upper surface by the presence of relatively incompetent and therefore nonbrittle sediment. In contrast, the lower limit of seismic activity may be bounded by hot middle crust at ~10 km depth, where ductile deformation precludes seismogenesis. Sections B and E (Fig. 14) show the depth distribution of the E-W–trending strike-slip events around 24°34′N (southern end of the profiles). The NE-SW–trending belt does show well in the cross section, with only a few events >30 km in Figure 14B, C. No evidence exists for a shallow-dipping active slip plane bounding the basin to the north on the basis of seismicity. Whatever fault motion we can confirm is either diffused or concentrated in a narrow depth range, probably between the bottom of the sedimentary layer and the top of the basement, judging from the rheological properties of these materials.

The events >50 km deep under the basin axis are interpreted as thrust earthquakes, consistent with their association with the Ryukyu subduction zone, which is now starting under northern Taiwan by lateral motion of the Philippine Sea plate into a tear in the passive margin lithosphere of southern China (Lallemand et al., 2001). However, analysis of earthquakes shallower than 20 km from the nearby Okinawa Trough shows a dominant extensional character, with extension perpendicular to the strike of the trough, i.e., NW-SE. These shallow earthquakes form an offshore continuation of the shallow events seen under the Ilan Basin, which are similarly interpreted as being extensional. No strong evidence exists from earthquakes to support the presence of a currently active major south-dipping detachment (e.g., the Lishan Fault). However, if the major extensional fault is shallow dipping, then it is too shallow to store elastic stresses and to be seismogenic under the northern part of the Ilan Plain. Deeper faulting under the southern edge of the basin is consistent with these asymmetric structural models. Strike-slip faulting in the southeast basin may be interpreted as part of the strain accommodation related to the bend in the tectonic fabric from a N-S orientation in central Taiwan to an E-W orientation in the Ryukyu Arc. The strain observed indicates motion of the southern margin

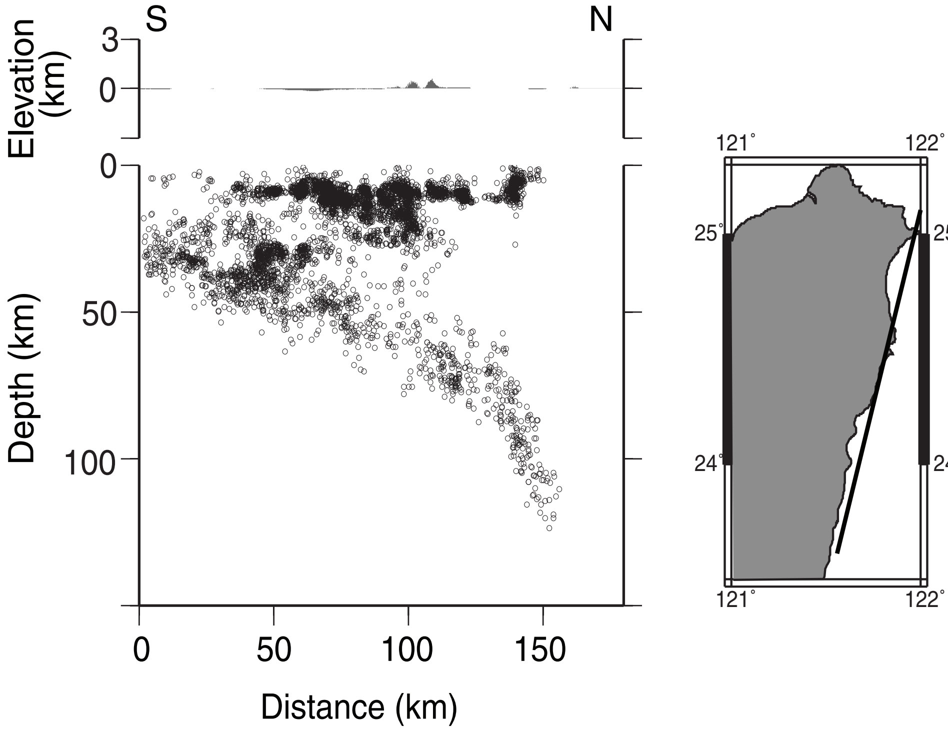

Figure 12. Cross section off the east coast of Taiwan, showing recent seismicity down to 150 km depth. The location of the section is shown as a black line on the map (right). Seismicity divides broadly into the shallow seismicity seen in detail in Figures 13 and 14, and the well-defined north-dipping Benioff zone of the Ryukyu Arc.

of the Ilan Basin to the ESE. The sense of motion is the opposite of that expected from the bending of the structural fabric, but it is consistent with the lateral motion of orogenic crust away from the Taiwan mountains toward the Ryukyu Trench, as might be predicted for orogenic collapse driven by a change in stresses triggered by generation of that trench.

GEODYNAMIC EVOLUTION

Additional constraints on the nature of current tectonic strain are provided by global positioning system (GPS) monitoring of the region. Here we consider the motions reconstructed by Chang et al. (2003), as shown in Figure 15. Relative to stable southern China the ranges north of the Ilan Basin are moving slowly to the northwest (~10–15 mm/yr), effectively a continuation of the west-directed thrusting that characterizes most of Taiwan, albeit slightly rotated clockwise in this particular area. In contrast, GPS locations in the Ilan Basin itself are moving almost due east, while the basement around Suao on the southern boundary is being displaced toward the southeast at 15–20 mm/yr. The net result indicates motion of the Hsüehshan and Backbone Ranges away from one another, consistent with the seismic evidence for extension across the basin. The eastward motion of the Ilan Basin shows the same sense of motion as the strike-slip fault data derived from the fault plane solutions of the seismic data. It should be noted that the major strike-slip structures (Fig. 11) are south of the GPS stations on the Ilan Plain. The GPS data thus indicate a broader zone of crustal extrusion than that based on the seismology alone, implying extrusion of this crustal block toward the Okinawa Trough. We do recognize the importance of the strike-slip zone resolved by the seismic data and note that GPS motions are more south-oriented, directly toward the trench, south of that lineament.

The GPS motion data can be understood in the context of the tectonic setting that is characterized by E-W compression in central Taiwan, contrasting with N-S subduction to the east along the Ryukyu Trench. In practice the Ryukyu Trench provides a free edge, allowing the southward motion of crustal blocks in the Ryukyu forearc, compared with the compression by the Luzon-China collision (Fig. 16). If Taiwan is considered an arc-continent collision orogen that is progressively migrating along the Chinese margin toward the southwest, then the passive-margin units that are compressed and uplifted by collision may then collapse and extend, once the restraining buttress of the Philippine Sea plate has been removed and subduction with the opposite polarity is initiated. The load of the Taiwan orogen causes flexure of the underlying Chinese continental crust (Yu and Chou, 2001; Lin and Watts, 2002; Lin et al., 2003). Where that load slides southeastward away from the margin's edge in northern Taiwan, the continental crust quickly rebounds and regains much of its normal thickness (Rau and Wu, 1995). Thus SE-directed motion of the basement south of the Ilan Basin reflects collapse of the flank of the Taiwan orogen and motion of the Backbone Range toward the Ryukyu Trench. Extension in the Okinawa Trough, driven by southward motion of the Ryukyu forearc toward the trench also provides space for

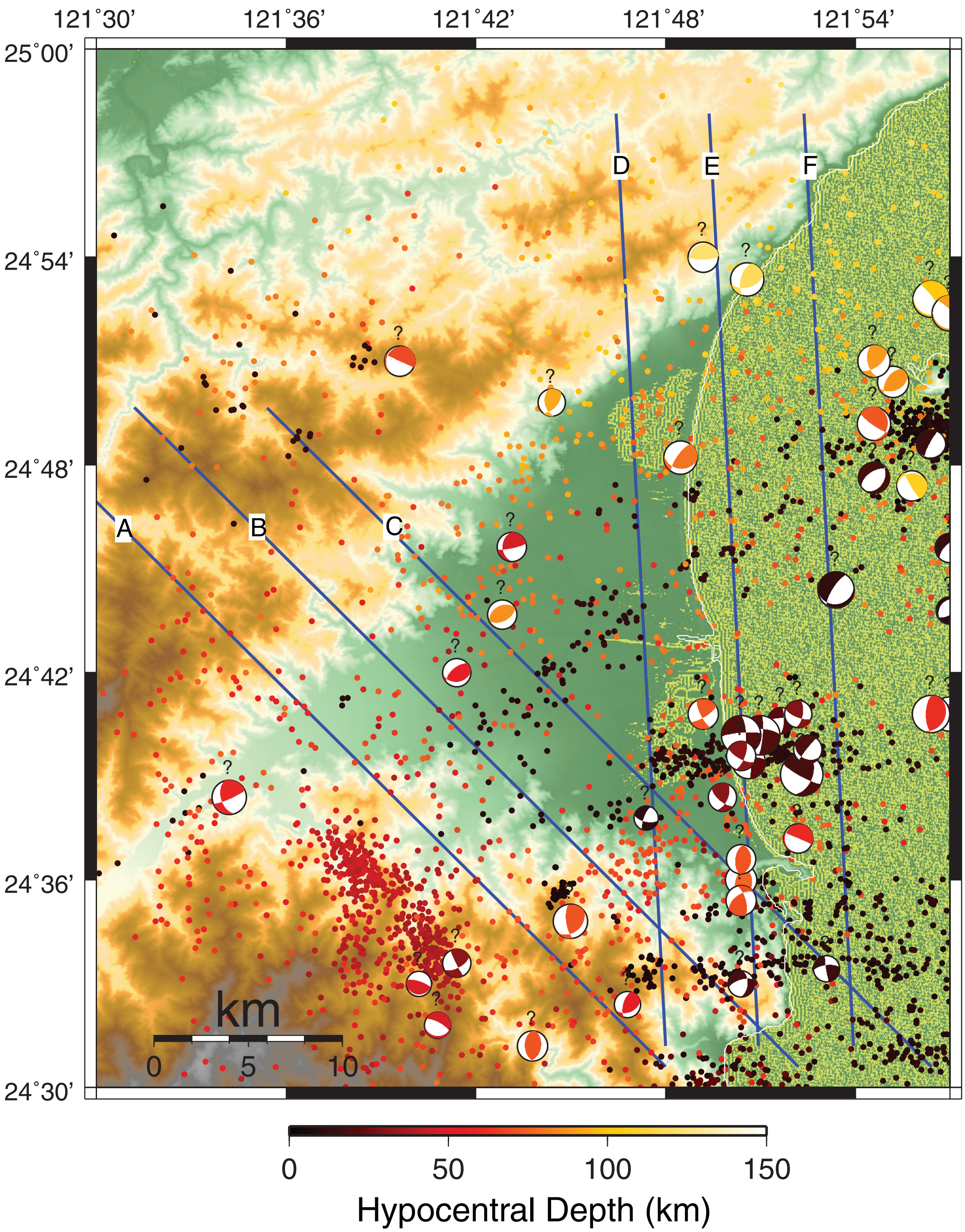

Figure 13. Map showing the location of earthquake hypocenters around the Ilan Basin, with the dominant extensional character of recent events at depths <20 km, whereas deeper events are thrust motions linked to the Ryukyu subduction zone and the Taiwan collision. Parallel lines A, B, C and D, E, F denote cross sections shown in Figure 14.

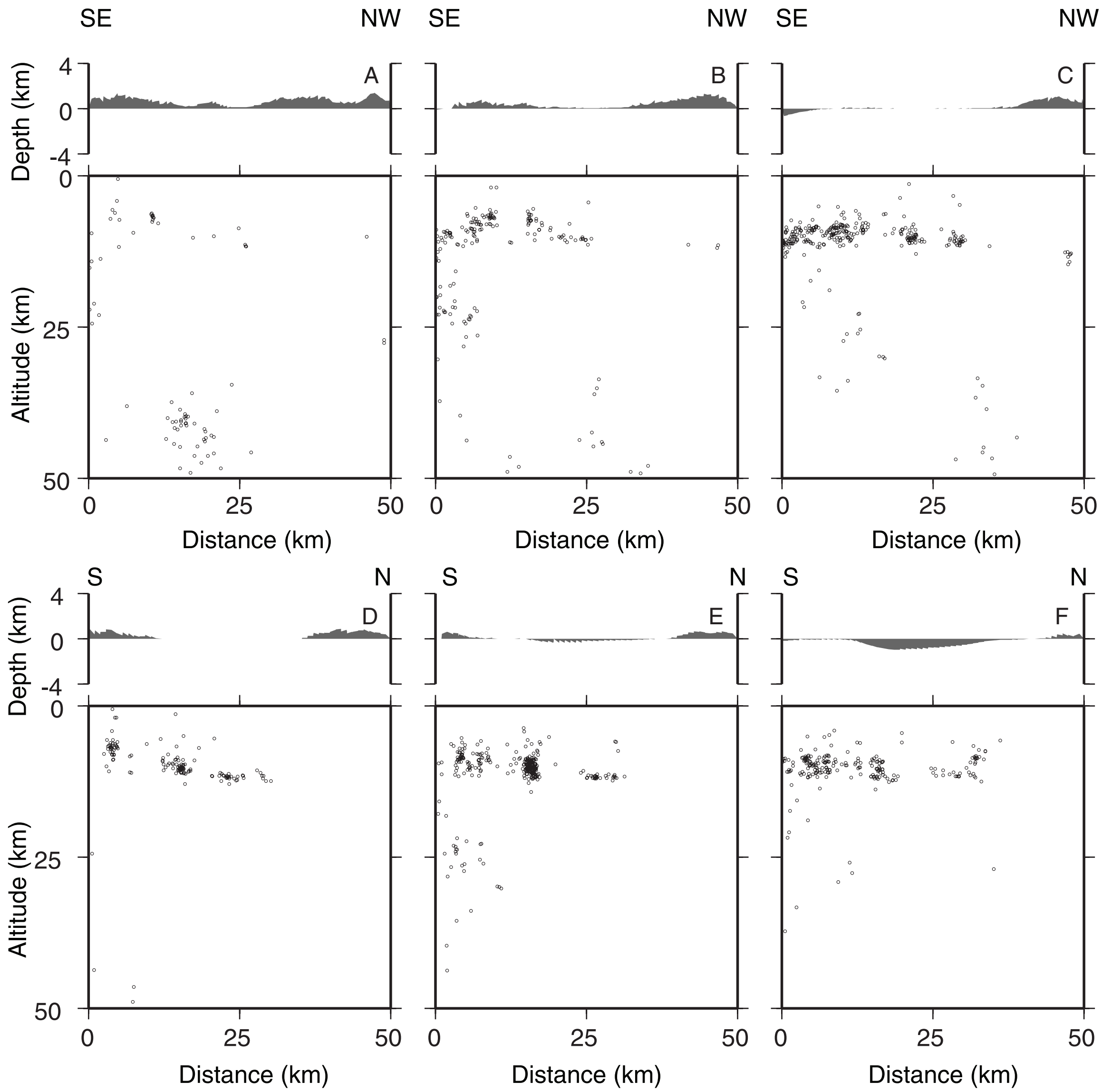

Figure 14. Cross sections down to 50 km depth across the basin show concentrated seismicity ~13–8 km depth. Those in the 13–50 km range are evidently associated with collision of the Philippine Sea and Eurasian plates, and the subduction events are at depths >50 km in this region. Section locations are shown in Figure 13.

the eastward motion of material in the Ilan Basin, driven by the gravitational potential of the thickened crust in central Taiwan. This motion is partially accommodated by strike-slip tectonism as seen in the seismic data, as well as by extension, especially that focused on the major fault bounding the Ilan Plain to the north, inferred to be the Lishan Fault, reversed in direction in comparison with its thrust sense in the Central Ranges.

DISCUSSION

The fact that the Lishan Fault can be traced along strike from a major thrust fault into an extensional detachment is consistent with the extension in the Ilan Basin being the product of post-orogenic collapse, triggered by subduction polarity reversal, as argued by Teng (1996), and not the result of extension propagating from the Okinawa Trough, driven by trench forces. The extensional fault that controls the Ilan Basin does not represent a westward propagating rift of oceanic origin cutting across the older orogenic fabric, but rather a reversal of motion on thrusts as compressional stresses are released toward the northern end of the orogen. The major bounding fault can be clearly traced as an extension of the Lishan Fault, which is a major thrust structure in the Central Ranges but is overturned and moving as an extensional structure where it reaches the Ilan Plain. The initiation of

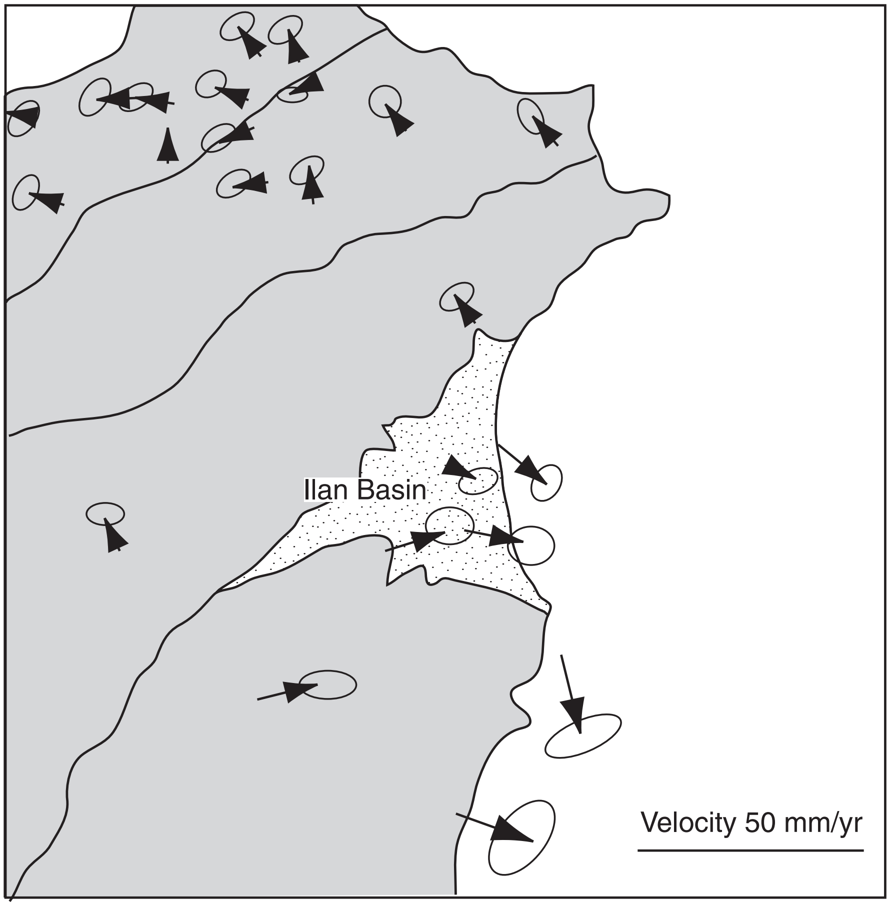

Figure 15. Map showing the motions of crustal blocks around the Ilan Basin relative to stable Eurasia, recorded by Chang et al. (2003) using GPS methods over the period 1990–1995.

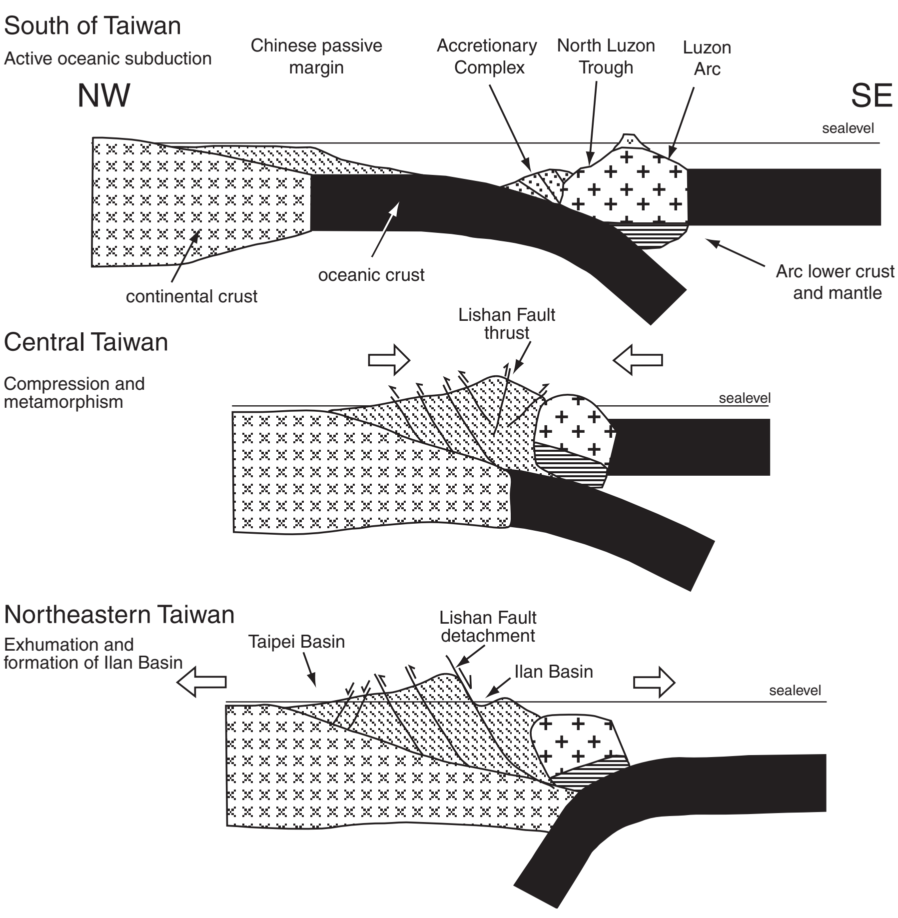

Figure 16. Schematic depiction of the origin of the Ilan Basin as a result of gravitational collapse of the Taiwan Central Ranges during a SW-migrating collision of the Luzon Arc and mainland China.

the Ryukyu Trench removes the compressive force of the Philippine Sea plate from the orogen and allows the edifice to extend as the trench provides a free edge toward which material can be displaced. In turn this suggests that at least the southwestern end of the Okinawa Trough has also formed as a result of migrating arc-continent collision and subsequent orogenic collapse and is not generated by subduction slab rollback (cf. Suppe, 1984). This is an important revision of the generally held belief that the Okinawa Trough is formed by trench forces, principally rollback of the trench, much as suggested for the Mariana Trough or the Lau Basin (e.g., Hawkins, 1974). However, in the rollback model the presence of the westernmost propagating end of the rift at the northern tip of Taiwan would be coincidental, whereas rifting related to collision and subduction polarity reversal would predict this position. In practice, little evidence exists for active rift propagation. The Okinawa Trough is not V-shaped as seen in other western Pacific basins, where a propagating rift culminates in seafloor spreading. The Okinawa Trough appears to be opening to the west, yet the older eastern parts of the basin are no wider than that closest to Taiwan. In the Okinawa Trough, rifting is followed by a cessation of extension, whereas in contrast rollback and arc rifting are normally followed by further extension in the form of seafloor spreading.

Evidence that the westward migration of the Okinawa Trough is matched by arc migration was provided by Shinjo (1999), who noted that middle Miocene volcanic rocks from the southern Ryukyu Arc are not subduction related but instead are similar to intraplate volcanism seen in China. Such an observation implies that the Ryukyu Arc is new and that the subduction-related Ryukyu volcanic front has propagated into the area since that time. This hypothesis is also supported by the geochemistry of recent volcanic rocks from the southernmost Okinawa Trough (Chung et al., 2000). In a collapse model the Okinawa Trough becomes increasingly younger to the south, the opposite of the rollback model in which the Okinawa Trough spreading centers are propagating into the basin away from Taiwan.

It is noteworthy that active magmatism and faulting that cuts right to the seafloor in the Okinawa Trough is restricted to that part of the basin closest to Taiwan (Sibuet et al., 1998). In contrast, middle to late Miocene (6–9 Ma) extension ages are recorded in the northern Okinawa Trough (Letouzey and Kimura, 1985). The northern Okinawa Trough thus is either the remnant of an earlier arc-continent collision, as favored by Clift et al. (2003), or has a separate origin from that part of the basin closer to Taiwan. The basement of the southern Okinawa Trough is inferred to be the extended remnants of the Taiwan orogen, equivalent to the Backbone and Hsüehshan Ranges. The recognition of a continuous Taiwan-Sinzi folded zone under the SE edge of the East China Sea (Hsiao et al., 1999) would suggest a continuous migration of the orogen from Sinzi at ca. 12 Ma to present-day Taiwan. Volcanism is the manifestation of the new arc volcanic front to the Ryukyu subduction zone, which overlies the nonvolcanic forearc ridge only in the central and northern Ryukyu Arc, where active extension has ceased.

Here we propose that the Ilan Basin can best be understood in the context of a migrating arc collision, and especially as the culmination of gravitational collapse of the resultant orogen, having taken place over relatively short periods of geologic time (Fig. 17). Collision of the modern Taiwan section of the Luzon Arc with China is thought to have begun ca. 6–9 Ma (e.g., Dorsey, 1988; Teng, 1990; Sibuet et al., 2002; Malavieille et al., 2002; Huang et al., 2006) and is already finished and in a state of rapid exhumation around the Ilan Basin. Byrne and Crespi (1997) reported extension throughout the Backbone and Central Ranges. The stronger extension seen around the Ilan Basin can be understood as an extension of this, made possible as the new Ryukyu Trench form, removing the compressive stresses of collision and allowing the flank of the Taiwan orogen to move laterally into that space.

Figure 18 shows the relationship between tectonically driven rock uplift rates and exhumation rates in Taiwan, assuming that "hard collision" in northern Taiwan initiated ca. 5 Ma, whereas in the south hard collision between the Luzon Arc and China is just starting at the modern coast. Initial collision between the Luzon forearc and the Chinese margin begins farther south, with the development of an accretionary prism, which progressively overthrusts the North Luzon Trough (forearc basin; Lundberg et al., 1997). Regional trends in rock uplift rates can be determined from the current elevations and the age of the collision, together with estimates for the amount of exhumation derived from the metamorphic-grade and fission-track data (e.g., Dadson et al., 2003). Although in some areas modern rates of uplift have been determined by dating terraces (e.g., Lin, 1969; Peng et al., 1977; Vita-Finzi and Lin, 1998), these terraces are necessarily limited to the coastal regions, mostly in the Coastal Ranges of eastern Taiwan.

Exhumation rates driven by erosion reach a peak in the south of the island, because rates of rock uplift are highest during the most intense period of collisional compression between Luzon and China; these are partly balanced by erosion driven largely by precipitation but also by tectonic extension (Crespi et al., 1996; Teng et al., 2000). Exhumation and vertical uplift rates decrease abruptly toward the northern end of the Central Ranges, especially around the Ilan Basin, although active motion along a detachment reversing the Lishan Fault causes increased exhumation in the Hsüehshan Range. The rates of burial and exhumation are some of the highest known on Earth. Exhumation rates at Nanga Parbat in the Pakistan Himalaya reach 5 mm/yr (Zeitler et al., 1993), slightly less than the rates seen in the Central Ranges (Dadson et al., 2003). Although exhumation rates are lower in the Hsüehshan Range, reaching >1.6 mm/yr adjacent to the Lishan Fault, these levels are still relatively high, far exceeding rates of 0.33 mm/yr in the Cascade Range of the northwestern United States (Reiners et al., 2003), somewhat more than the ~1 mm/yr found in the Alaska Range (Fitzgerald et al., 1993), and comparable to the 2.5–0.8 mm/yr measured by Tippett and Kamp (1993) in the southern Alps of New Zealand. Clearly arc-continent collision forms some of the most dynamic geology on the planet.

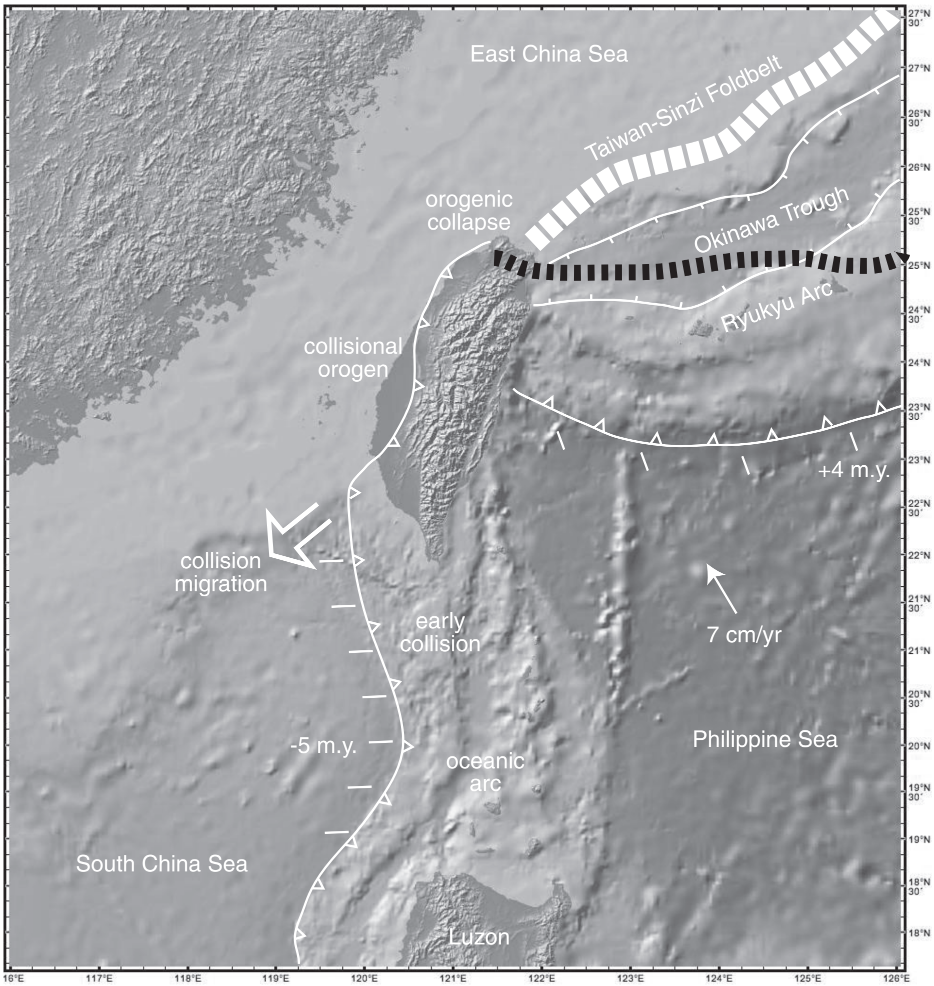

Figure 17. Shaded bathymetric map of the Taiwan region, showing the collisional orogen, the opposing subduction polarities, and the Okinawa Trough opening in the wake of orogenic collapse. The numbered lines adjacent to the plate boundary show the inferred time of peak arc collision between Luzon and China. Map is labeled to show the different stages of arc-continent collision along strike. Wide white dashed line shows location of the Taiwan-Sinzi Fold Belt, interpreted as remnants of the former collisional orogen. Black dashed line shows the location of the modern arc volcanic front, focused by extension in the Okinawa Trough close to Taiwan.

CONCLUSIONS

A variety of geological and geophysical data demonstrates active extension along a NNW-SSE axis across the Ilan Basin of northern Taiwan. The structure of the basin appears to be largely controlled by a SE-dipping detachment fault, likely dipping at ~30°, that causes uplift of the Hsüehshan Range to the north of the basin and preferential fast subsidence of the northern Ilan Basin. Apatite fission-track ages confirm geomorphic evidence for faster exhumation of the northern margin of the basin, reaching rates of at least 1.6 ± 0.3 km/m.y. The main basin-bounding extensional fault is mapped as a continuation of the Lishan Fault, a major thrust structure from central Taiwan. The southern Backbone Range is shown by seismic and GPS data to be moving southeast toward the newly formed western Ryukyu Trench. Formation of a free edge in the trench and release of the E-W compressive stresses allow the Taiwan orogen to collapse in the Ilan Basin–Okinawa Trough region. Because the Taiwan orogen is migrating to the southwest along the passive margin of southern China, we suggest that the extension and associated basin formation must also move in this direction. Although the Ilan Basin was formed by the start of collapse onshore, the process reached its culmination offshore in the Okinawa Trough, indicating that at least some of this basin has formed as a result of collision and not by trench rollback forces as previously believed (cf. Suppe, 1984). We propose that mountain building and rifting of the Ilan Plain and the Okinawa Trough are all results of a single common process, arc-continent collision, rather than being the unique interaction of a collisional orogen and a propagating backarc rift. Like the Alboran Sea in the western Mediterranean the Ilan-Okinawa Trough shows how far postorogenic collapse may drive extension and basin formation (e.g., Platt and Vissers, 1989), although in this case without the need to invoke delamination of the mantle lithosphere.

Because arc-continent collision is a common process in the plate-tectonic cycle we anticipate that collapse basins similar to the Ilan Basin should be a common feature and should be recognizable in ancient collision zones. Although the Ordovician South Mayo Trough of the Irish Caledonides has been interpreted to be such a basin (e.g., Clift et al., 2003), the scarcity of other examples likely reflects a lack of understanding of existing sequences rather than the absence of gravitational collapse in ancient arc collisional events.

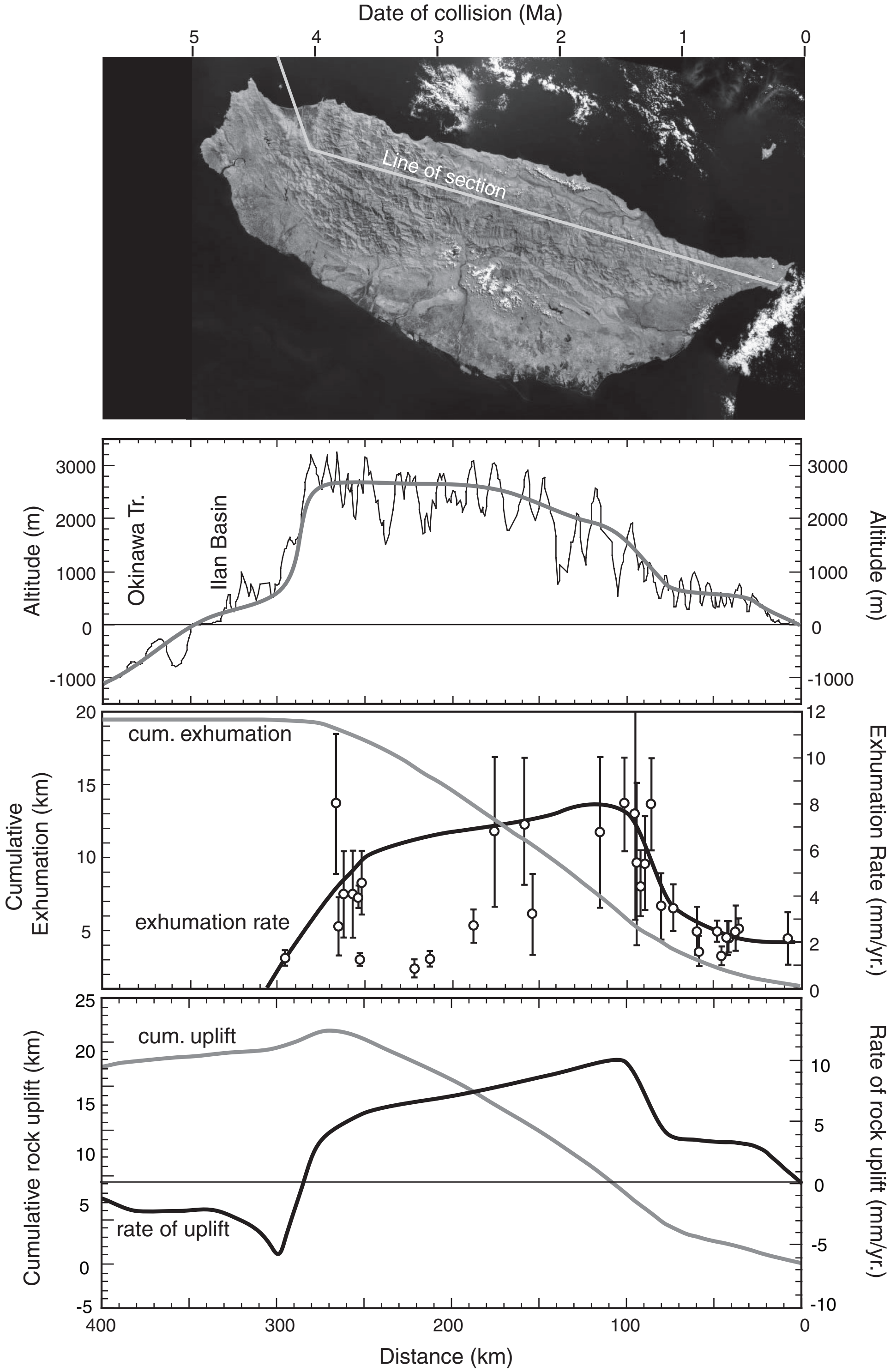

Figure 18. Summary of the trends in rock uplift and exhumation rate along the length of the island of Taiwan, depicted also as a time progression of hard collision during initial arc-continent collision passing into extension, exhumation, and collapse, culminating in formation of the Okinawa Trough. Exhumation rates are from Dadson et al. (2003). Gray line shows long-wavelength topography.

ACKNOWLEDGMENTS

P.C. thanks the University of Aberdeen, College of Physical Sciences; the Alexander von Humboldt Foundation; and the Joint Oceanographic Institutions for contributions to the cost of this research. A.T.L. is grateful for financial support for conducting fieldwork from an NSC (Taiwan) grant of 93–2116-M-008–001. F.T.W. acknowledges support from the U.S. National Science Foundation's Continental Dynamics Program. We thank Don Fisher, Neil Lundberg, Dave Topping, and Patrick Barnard for their helpful reviews, as well as editor Dave Scholl for his help in improving this manuscript.

REFERENCES CITED

Barr, T.D., and Dahlen, F.A., 1988, Thermodynamic efficiency of brittle frictional mountain building: Science, v. 242, p. 749–752, doi: 10.1126/science.242.4879.749.

Byrne, T., and Crespi, J., 1997, Kinematics of the Taiwan arc-continent collision and implications for orogenic process: Tapei, Taiwan, International Conference and Sino-American Symposium on Tectonics of East Asia, p. 38.

Casey, J.F., and Dewey, J.F., 1984, Initiation of subduction zones along transform and accreting plate boundaries, triple-junction evolution, and forearc spreading centres—Implications for ophiolitic geology and obduction, *in* Gass, I.G., et al., Ophiolites and Oceanic Lithosphere: Geological Society [London] Special Publication 13, p. 269–290.

Chang, C.-P., Chang, T.-Y., Angelier, A., Kao, H., Lee, J.-C., and Yu, S.-B., 2003, Strain and stress field in Taiwan oblique convergent system: Constraints from GPS observation and tectonic data: Earth and Planetary Science Letters, v. 214, p. 115–127, doi: 10.1016/S0012-821X(03)00360-1.

Chemenda, A.I., Yang, R.K., Hsieh, C.H., and Groholsky, A.L., 1997, Evolutionary model for the Taiwan collision based on physical modeling: Tectonophysics, v. 274, p. 253–274, doi: 10.1016/S0040-1951(97)00025-5.

Chen, C.H., 1984, Determination of lower greenschist facies boundary by K-mica-chlorite crystallinity in the Central Range, Taiwan: Proceedings of the Geological Society of China, v. 27, p. 41–53.

Chen, J., and Jahn, B.M., 1998, Crustal evolution of southeastern China: Nd and Sr isotopic evidence: Tectonophysics, v. 284, p. 101–133, doi: 10.1016/S0040-1951(97)00186-8.

Chung, S.L., Wang, S.L., Shinjo, R., Lee, C.S., and Chen, C.H., 2000, Initiation of arc magmatism in an embryonic continental rifting zone of the southernmost part of Okinawa Trough: Terra Nova, v. 12, p. 225–230, doi: 10.1046/j.1365-3121.2000.00298.x.

Clark, M.B., Fisher, D., and Lu, C.-Y., 1993, The Hsueshan Range of Taiwan: A crustal scale pop-up structure: Tectonics, v. 12, p. 205–217.

Clift, P.D., and Vannucchi, P., 2004, Controls on tectonic accretion versus erosion in subduction zones: Implications for the origin and recycling of the continental crust: Reviews of Geophysics, v. 42, p. RG2001, doi: 10.1029/2003RG000127.

Clift, P.D., Schouten, H., and Draut, A.E., 2003, A general model of arc-continent collision and subduction polarity reversal from Taiwan and the Irish Caledonides, *in* Larter, R.D., and Leat, P.T., eds., Intra-Oceanic Subduction Systems; Tectonic and Magmatic Processes: Geological Society [London] Special Publication 219, p. 81–98.

Crespi, J., Chan, Y.C., and Swaim, M., 1996, Synorogenic extension and exhumation of the Taiwan hinterland: Geology, v. 24, p. 247–250, doi: 10.1130/0091-7613(1996)024<0247:SEAEOT>2.3.CO;2.

Dadson, S., Hovius, N., Chen, H., Dade, W.B., Hsieh, M.L., Willett, S., Hu, J.C., Horng, M.J., Chen, M.C., Stark, C.P., Lague, D., and Lin, J.C., 2003, Links between erosion, runoff variability and seismicity in the Taiwan orogen: Nature, v. 426, p. 648–651, doi: 10.1038/nature02150.

Davis, D.W., Sewell, R.J., and Campbell, S.D.G., 1997, U-Pb dating of Mesozoic igneous rocks from Hong Kong: Geological Society [London] Journal, v. 154, p. 1067–1076.

Dorsey, B.J., 1988, Provenance evolution and un-roofing history of modern arc-continent collision: Evidence from petrography of Plio-Pleistocene sandstones, eastern Taiwan: Journal of Sedimentary Petrology, v. 58, p. 208–218.

Fitzgerald, P.G., Stump, E., and Redfield, T.F., 1993, Late Cenozoic uplift of Denali and its relation to relative plate motion and fault morphology: Science, v. 259, p. 497–499, doi: 10.1126/science.259.5094.497.

Galbraith, R.F., 1990, The radial plot: Graphical assessment of spread in ages: Nuclear Tracks, v. 17, p. 207–214.

Green, P.F., Duddy, I.R., Laslett, G.M., Hegarty, K.A., Gleadow, A.J., and Lovering, J., 1989, Thermal annealing of fission-tracks in apatite; 4, Quantitative modeling techniques and extension to geological timescales: Chemical Geology, v. 79, p. 155–182.

Hawkins, J.W., 1974, Geology of the Lau Basin, a marginal sea behind the Tonga arc, *in* Burk, C.A., and Drake, C.L., eds., The Geology of Continental Margins: New York, Springer-Verlag, p. 505–520.

Hsiao, L.-Y., Lin, K.-A., Huang, S.T., and Teng, L.S., 1999, Structural characteristics of the southern Taiwan-Sinzi folded zone: Petroleum Geology of Taiwan, v. 32, p. 133–153.

Hsu, S.-K., and Sibuet, J.-C., 1995, Is Taiwan the result of arc-continent or arc–arc collision?: Earth and Planetary Science Letters, v. 136, p. 315–324, doi: 10.1016/0012-821X(95)00190-N.

Huang, C.Y., Yuan, P.B., Lin, C.W., and Wang, T.K., 2000, Geodynamic processes of Taiwan arc-continent collision and comparison with analogs in Timor, Papua New Guinea, Urals and Corsica: Tectonophysics, v. 325, p. 1–21, doi: 10.1016/S0040-1951(00)00128-1.

Huang, C.Y., Yuan, P.B., and Tsao, S.H., 2006, Temporal and spatial records of active arc-continent collision in Taiwan: A synthesis: Geological Society of America Bulletin, v. 118, p. 274–288, doi: 10.1130/B25527.1.

Hurford, A.J., 1990, Standardization of fission-track dating calibration: Recommendation by the Fission-track Working Group of the IUGS Subcommission on Geochronology: Chemical Geology, v. 80, p. 177–178.

Konstantinovskaya, E.A., 1999, Geodynamics of island arc–continent collision in the western Pacific margin: Geotectonics, v. 33, p. 15–34.

Kusznir, N.J., Marsden, G., and Egan, S.S., 1991, A flexural cantilever simple shear/pure shear model of continental extension, *in* Roberts, A.M., et al., eds., The Geometry of Normal Faults: Geological Society [London] Special Publication 56, p. 41–61.

Kusznir, N.J., Roberts, A.M., and Morley, C.K., 1995, Forward and reverse modeling of rift basin formation, *in* Lambiase, J.J., ed., Hydrocarbon Habitat in Rift Basins: Geological Society [London] Special Publication 80, p. 33–56.

Lai, T.H., and Hsieh, M.L., 2003, Late-Quaternary vertical rock-movement rates of the coastal plains of Taiwan: Abstracts, Annual Meeting of Geological Society of China, p. 119.

Lallemand, S., Front, Y., Bijwaard, H., and Kao, H., 2001, New insights on 3-D plates interaction near Taiwan from tomography and tectonic implications: Tectonophysics, v. 335, p. 229–253, doi: 10.1016/S0040-1951(01)00071-3.

Lee, J.C., Chu, H.-T., Angelier, J., Chan, Y.-C., Hu, J.-C., Lu, C.-Y., and Rau, R.-J., 2002, Geometry and structure of northern surface ruptures of the 1999 Mw = 7.6 Chi-Chi, Taiwan earthquake: Influence from inherited fold belt structures: Journal of Structural Geology, v. 24, p. 173–192, doi: 10.1016/S0191-8141(01)00056-6.

Leeder, M.R., and Gawthorpe, R.L., 1987, Sedimentary models for extensional tilt-block/half-graben basins, *in* Coward, M.P., et al., eds., Continental Extensional Tectonics: Geological Society [London] Special Publication 28, p. 139–152.

Letouzey, J., and Kimura, M., 1985, Okinawa Trough genesis; structure and evolution of a backarc basin developed in a continent: Marine and Petroleum Geology, v. 2, p. 111–130, doi: 10.1016/0264-8172(85)90002-9.

Lin, A.T., and Watts, A.B., 2002, Origin of the West Taiwan basin by orogenic loading and flexure of a rifted continental margin: Journal of Geophysical Research, v. 107, p. 2185, doi: 10.1029/2001JB000669.

Lin, A.T., Watts, A.B., and Hesselbo, S.P., 2003, Cenozoic stratigraphy and subsidence history of the South China Seamargin in the Taiwan region: Basin Research, v. 15, p. 453–478, doi: 10.1046/j.1365-2117.2003.00215.x.

Lin, C.C., 1969, Holocene geology of Taiwan: Acta Geologica Taiwanica, v. 13, p. 83–126.

Liu, T.K., Chen, Y.G., Chen, W.S., and Jiang, S.H., 2000, Rates of cooling and denudation of the Early Penglai Orogeny, Taiwan, as assessed by fission-track constraints: Tectonophysics, v. 320, p. 69–82, doi: 10.1016/S0040-1951(00)00028-7.

Liu, T.K., Hsieh, S., Chen, Y.G., and Chen, W.S., 2001, Thermo-kinematic evolution of the Taiwan oblique-collision mountain belt as revealed by zircon fission track dating: Earth and Planetary Science Letters, v. 186, p. 45–56, doi: 10.1016/S0012-821X(01)00232-1.

Lo, C.H., and Yu, T.F., 1996, 40Ar/39Ar dating of high-pressure rocks in the Tananao basement complex, Taiwan: Journal of the Geological Society of China, v. 39, p. 13–30.

Lu, C.-Y., and Hsü, K.-J., 1992, Tectonic evolution of the Taiwan mountain belt: Petroleum Geology of Taiwan, v. 27, p. 21–46.

Lundberg, N., Reed, D.L., Liu, C.-S., and Lieske, J., 1997, Forearc-basin closure and arc accretion in the submarine suture zone south of Taiwan: Tectonophysics, v. 274, p. 5–23, doi: 10.1016/S0040-1951(96)00295-8.

Malavieille, J., Lallemand, S.E., Dominguez, S., Deschamps, A., Lu, C.-Y., Liu, C.-S., and Schnurle, P., and the ACT scientific crew, 2002, Arc-continent collision in Taiwan: New marine observations and tectonic evolution, *in* Byrne, T.B., and Liu, C.-S., eds., Geology and Geophysics of an Arc-Continent Collision, Taiwan: Geological Society of America Special Paper 358, p. 187–211.

Peng, T.-H., Li, Y.-H., and Wu, F.T., 1977, Tectonic uplift rates of the Taiwan Island since the early Holocene, *in* Ho, C.S., A Special Volume Dedicated to Biq Chingchang on the Occasion of His Retirement: Taipei, Taiwan, Geological Society of China Memoir 2, p. 57–69.

Platt, J.P., and Vissers, R.L.M., 1989, Extensional collapse of thickened continental lithosphere: A working hypothesis for the Alboran sea and Gibraltar arc: Geology, v. 17, p. 540–543, doi: 10.1130/0091-7613(1989)017<0540:ECOTCL>2.3.CO;2.

Rau, R.-J., and Wu, F.T., 1995, Tomographic imaging of lithospheric structures under Taiwan: Earth and Planetary Science Letters, v. 133, p. 517–532, doi: 10.1016/0012-821X(95)00076-O.

Reiners, P.W., Ehlers, T.A., Mitchell, S.G., and Montgomery, D.R., 2003, Coupled spatial variations in precipitation and long-term erosion rates across the Washington Cascades: Nature, v. 426, p. 645–647, doi: 10.1038/nature02111.

Roberts, A.M., Yielding, G., Kusznir, N.J., Walker, I., and Dorn-Lopez, D., 1993, Mesozoic extension in the North Sea: Constraints from flexural backstripping, forward modeling and fault populations, *in* Parker, J.R., ed., Petroleum Geology of NW Europe: Geological Society [London], Proceedings of the 4th Conference, p. 1123–1136.

Rudnick, R.L., and Fountain, D.M., 1995, Nature and composition of the continental crust; a lower crustal perspective: Reviews of Geophysics, v. 33, p. 267–309, doi: 10.1029/95RG01302.

Shinjo, R., 1999, Geochemistry of high Mg andesites and the tectonic evolution of the Okinawa Trough–Ryukyu Arc system: Chemical Geology, v. 157, p. 69–88, doi: 10.1016/S0009-2541(98)00199-5.

Shyu, J.B.H., Sieh, K., Chen, Y.G., and Liu, C.S., 2005, Neotectonic architecture of Taiwan and its implications for future large earthquakes: Journal of Geophysical Research, v. 110, p. B08402, doi: 10.1029/2004JB003251.

Sibuet, J.-C., and Hsu, S.K., 1997, Geodynamics of the Taiwan arc–arc collision: Tectonophysics, v. 274, p. 221–251, doi: 10.1016/S0040-1951(96)00305-8.

Sibuet, J.-C., Deffontaines, B., Hsu, S.K., Thareau, N., Le Formal, J.P., and Liu, C.S., 1998, Okinawa Trough backarc basin; early tectonic and magmatic evolution: Journal of Geophysical Research, v. 103, p. 30,245–30,267, doi: 10.1029/98JB01823.

Sibuet, J.-C., Hsu, S.K., Le Pichon, X., le Formal, J.P., Reed, D., Moore, G., and Liu, C., 2002, East Asia plate tectonics since 15 Ma: Constraints from the Taiwan region: Tectonophysics, v. 344, p. 103–134, doi: 10.1016/S0040-1951(01)00202-5.

Suppe, J., 1981, Mechanics of mountain building and metamorphism in Taiwan, *in* Ho, C.S., and Ernst, W.G., Papers Presented at the ROC-USA Seminar on Plate Tectonics and Metamorphic Geology: Taipei, Taiwan, Geological Society of China Memoir 4, p. 67–89.

Suppe, J., 1984, Kinematics of arc-continent collision, flipping of subduction, and backarc spreading near Taiwan, *in* Tsan, S.F., et al., eds., A Special Volume Dedicated to Chun-Sun Ho on the Occasion of His Retirement: Geological Society of China Memoir 6, p. 21–33.

Suppe, J., Wang, Y., Liou, J.G., and Ernst, W.G., 1976, Observation of some contacts between basement and Cenozoic cover in the Central Range, Taiwan: Proceedings of the Geological Society of China, v. 19, p. 59–70.

Tagami, T., Galbraith, R.F., Yamada, G.M., and Laslett, G.M., 1998, Revised annealing kinetics of fission-tracks in zircon and geological implications, *in* Van den Haute, P., and De Corte, F., eds., Advances in Fission-track Geochronology: Amsterdam, Kluwer Academic Press, p. 99–112.

Teng, L.S., 1990, Geotectonic evolution of late Cenozoic arc-continent collision in Taiwan: Tectonophysics, v. 183, p. 57–76, doi: 10.1016/0040-1951(90)90188-E.

Teng, L.S., 1996, Extensional collapse of the northern Taiwan mountain belt: Geology, v. 24, p. 949–952, doi: 10.1130/0091-7613(1996)024<0949:ECOTNT>2.3.CO;2.

Teng, L.S., and Lee, C.-T., 1996, Geodynamic appraisal of seismogenic faults in northeast Taiwan: Proceedings of the Geological Society of China, v. 39, p. 125–142.

Teng, L.S., Wang, Y., Tang, C.-H., Huang, C.-Y., Huang, T.-C., Yu, M.-S., and Ke, A., 1991, Tectonic aspects of the Paleogene depositional basin of northern Taiwan: Proceedings of the Geological Society of China, v. 34, p. 313–336.

Teng, L.S., Lee, C.-T., Tsai, Y.-B., and Hsiao, L.-Y., 2000, Slab breakoff as a mechanism for flipping of subduction polarity in Taiwan: Geology, v. 28, p. 155–158, doi: 10.1130/0091-7613(2000)28<155:SBAAMF>2.0.CO;2.

Tippett, J.M., and Kamp, P.J.J., 1993, Fission-track analysis of the Late Cenozoic vertical kinematics of continental Pacific crust, South Island, New Zealand: Journal of Geophysical Research, v. 98, p. 16,119–16,148.

Vita-Finzi, C., and Lin, J.C., 1998, Serial reverse and strike slip on imbricate faults: The Coastal Range of east Taiwan: Geology, v. 26, p. 279–282, doi: 10.1130/0091-7613(1998)026<0279:SRASSO>2.3.CO;2.

von Huene, R., and Scholl, D.W., 1991, Observations at convergent margins concerning sediment subduction and the growth of continental crust: Reviews of Geophysics, v. 29, p. 279–316.

Waldhauser, F., 2001, HypoDD: A computer program to compute double-difference hypocenter locations: U.S. Geological Survey Open-File Report 01-113 (Menlo Park, California).

Waldhauser, F., and Ellsworth, W.L., 2000, A double-difference earthquake location algorithm: Method and application to the northern Hayward fault: Bulletin of the Seismological Society of America, v. 90, p. 1353–1368, doi: 10.1785/0120000006.

Wang, K.L., Chung, S.L., Chen, C.-H., Shinjo, R., Yang, T.F., and Chen, C.H., 1999, Post-collisional magmatism around northern Taiwan and its relation with opening of the Okinawa Trough: Tectonophysics, v. 308, p. 363–376, doi: 10.1016/S0040-1951(99)00111-0.

Wang, P.L., Lin, L.H., and Lo, C.H., 1998, 40Ar/39Ar dating of mylonitization in the Tananao schist, eastern Taiwan: Geological Society of China Journal, v. 41, p. 159–183.

Willett, S.D., Fisher, D., Fuller, C., Yeh, E.-C., and Lu, C.-Y., 2003, Erosion rates and orogenic-wedge kinematics in Taiwan inferred from fission-track thermochronometry: Geology, v. 31, p. 945–948, doi: 10.1130/G19702.1.

Wu, F.T., 1978, Recent tectonics in Taiwan: Journal of Physics of the Earth, v. 26, p. S265–S299.

Wu, F.T., Rau, R.J., and Salzberg, D.H., 1997, Taiwan tectonics: Thin-skinned or lithospheric collision: Tectonophysics, v. 274, p. 191–220, doi: 10.1016/S0040-1951(96)00304-6.

Yu, H.-S., and Chou, Y.-W., 2001, Characteristics and development of the flexural forebulge and basal unconformity of western Taiwan foreland basin: Tectonophysics, v. 333, p. 277–291, doi: 10.1016/S0040-1951(00)00279-1.

Zeitler, P.K., Chamberlain, C.P., and Smith, H.A., 1993, Synchronous anatexis, metamorphism and rapid denudation at Nanga Parbat (Pakistan Himalaya): Geology, v. 21, p. 347–350, doi: 10.1130/0091-7613(1993)021<0347:SAMARD>2.3.CO;2.

Manuscript Accepted by the Society 24 April 2007